Impaired Tooth Development In Periostin Deficient Mice

Dissertation

zur Erlangung des Doktorgrades des Fachbereiches Chemie
der Universität Hamburg

vorgelegt von

Andreja Brodarac

Hamburg, 2006

Chapter 1

Summary

Our lab has identified periostin in a screen designed to identify molecules that are potentially important for Schwann cell development. This implicated that periostin might have a role in migration, proliferation and differentiation of Schwann cells during peripheral nervous system (PNS) development.
The aim of this study was to elucidate the biological functions of the extracellular matrix protein, Periostin, by a gene deletion approach using homologous recombination in murine embryonic stem (ES) cells.
The targeting vector used to achieve homologous recombination was designed to delete parts of the periostin gene and fuse the β-galactosidase in frame to the open reading frame (orf) of periostin thereby inactivating the periostin gene. The construction of the targeting vector and homologous recombination were successful. Following the injection of mutant ES cells into blastocysts, chimeric animals were born that transmitted the mutant allel to their offspring. Mating of heterozygous offspring resulted in the generation of periostin null mice.
Unexpectedly, the analysis of the DRG in mutant embryos at E12 (embryonic day 12) did not reveal significant changes. Also surviving mutant animals showed no obvious defects in the PNS. However, closer examination of mutant mice revealed interesting abnormalities during postnatal life regarding tooth development.

Initial analysis had revealed that the number of living periostin null mice did not follow the regular Mendelian distribution but was decreased by approximately 25%. We found that these mutants died shortly after birth (between day 0 and day 3). Furthermore, the surviving mutants were smaller, showed a reduced body weight and were less fertile when kept on hard pellet food (normal nutrition). However, the body weight of the periostin deficient mice could almost be completely rescued by the administration of soft food that replaced the hard food nutrition after the tooth defects had been identified (see below).
As periostin expression had been found in the periodontal ligament (PDL) and the periosteum of adult mice (Horiuchi et al., 1999) and later studies revealed its wide expression in different regions of the teeth and surrounding tissues during embryonic

development and postnatal stages (Suzuki et al., 2004; Kruzynska-Frejtag et al, 2004), we focussed our analysis on these tissues and structures.

The analysis of newborn mutants revealed no significant changes in the structure of the skeleton. The development of cartilage and bone was comparable in periostin mutants versus wild type mice. Initial tooth development seemed normal in mutant animals despite of the early expression. However, postnatally periostin mutants developed a severe phenotype in the incisors.

In this study, I was able to provide evidence that the cause for the observed severe tooth phenotype of the periostin deficient mice is due to a decreased incisor eruption rate. Thus, in the mouse, periostin seems to be an important contributor for the maintenance and remodelling of the periodontal ligament (PDL) during incisor eruption throughout lifetime.

In unserem Labor wurde Periostin in einem „Screen“, der speziell dazu diente Moleküle mit einer möglichen Bedeutung für die Schwannzellentwicklung zu identifizieren, entdeckt. Dieser Umstand impliziert, dass Periostin Funktionen bei der Wanderung, Proliferation und Differenzierung von Schwannzellen während der Entwicklung des peripheren Nervensystems (PNS) übernehmen könnte.

Im Rahmen dieser Arbeit sollten die biologischen Funktionen von Periostin, das zu den extrazellulären Matrix Molekülen gehört, analysiert werden. Dazu sollte mittels homologer Rekombination in embryonalen Stammzellen (ES-Zellen) der Maus eine Inaktivierung des Gens erreicht werden.

Der dazu verwendete Vektor war so konstruiert, dass einerseits die β-Galactosidase an das Startcodon des Periostins fusioniert wurde und andererseits Gensequenzen deletiert wurden, die zu einer Inaktivierung des Periostins führen sollten.

Die Konstruktion des Vektors und die homologe Rekombination verliefen erfolgreich. Nach Injektion mutanter ES-Zellen in Blastozysten wurden chimäre Tiere geboren, die das mutante Allel an ihre Nachkommen weitergaben. Durch Verpaarung von heterozygoten Nachkommen wurden schließlich homozygote Mutanten erzeugt.

Für uns unerwartet, ergab eine Analyse der Schwannzellen in Mausembryonen am Tag 12 der Embryonalentwickling (E12) keine Auffälligkeiten in den Mutanten. Auch überlebende mutante Tiere zeigten keine abnorme Entwicklung des PNS nach der Geburt oder im Erwachsenenalter. Eine genaue Analyse der Mutanten offenbarte jedoch interessante Defekte in der Zahnentwicklung, die sich mit zunehmendem Alter verstärkten.

Bei der primären Charakterisierung der Mauslinie fiel zunächst auf, dass der Anteil der mutanten Tiere um ungefähr 25% unter dem nach Mendel zu erwartenden Zahlen lag. Es zeigte sich, dass die Tiere während der ersten Tage nach der Geburt verstarben (Tag 0 – Tag 3). Zusätzlich waren die überlebenden Mutanten kleiner und leichter und waren außerdem nahezu unfruchtbar, wenn sie unter normalen Bedingungen (Ernährung mit Trockenfutter) gehalten wurden. Nach Entdeckung des Zahndefekts (siehe unten) wurde das Trockenfutter durch Weichfutter ersetzt.

Interessanterweise konnten durch diese Maßnahme der Gewichtsverlust und die reduzierte Größe der Periostinmutanten fast gänzlich korrigiert werden.

Wegen der bereits beschriebenen Expression von Periostin im Periodontium und Periosteum während der Entwicklung sowie im adulten Organismus (Horiuchi et al., 1999; Suzuki et al., 2004; Kruzynska-Frejtag et al, 2004) haben wir uns bei der Charakterisierung der Mutation zunächst auf diese Gewebe und Strukturen konzentriert.

Eine Analyse der Skelettentwicklung ergab bei Neugeborenen keine signifikanten Unterschiede zwischen Mutanten und Kontrolltieren. Zum Untersuchungszeitpunkt waren sowohl Knorpel als auch Knochen normal entwickelt. Auch die frühe Zahnentwicklung zeigte keinerlei Auffälligkeiten und verlief in den Mutanten normal. Dies war für uns überraschend, da Periostin ja bereits früh in diesen Strukturen exprimiert wird. Postnatal entwickelten die Periostinmutanten jedoch einen schwerwiegenden Zahndefekt in den Nagezähnen.

Die Analysen, die in dieser Arbeit beschrieben werden, deuten darauf hin, dass die beobachteten Defekte in den Nagezähnen der Periostinmutanten durch eine verminderte Eruptionsrate der Nagezähne bedingt und erklärbar sind. Somit spielt Periostin bei Nagern eine wichtige Rolle bei der Zahneruption und hat wahrscheinlich weitere Funktionen im Peridontium, die möglicherweise auch in anderen Spezies konserviert sind.

Chapter 2

Introduction

2.1 The extracellular matrix

The extracellular matrix (ECM), which is secreted by adjacent cells, provides a structural support to cells and tissues. Over the past years, it has become evident that the ECM can instruct cells to perform specific functions through ECM-cell interactions. Thereby, the ECM can influence cellular behaviour during development and homeostasis and affect such diverse processes as cell migration, differentiation and pathological events.

The ECM can be found in several forms. In the connective tissue, ECM surrounds and binds the cells together. It can form the basal lamina, which separates different tissue type and most abundantly it is found in connective tissues such as bone, tendon and cartilage containing relatively few cells. Structure and function of each tissue is based on specific combination of matrix molecules.

In vertebrates, the ECM is composed of a complex mixture of fibrous collagens, proteoglycans and glycoproteins (Fig. 2.1).

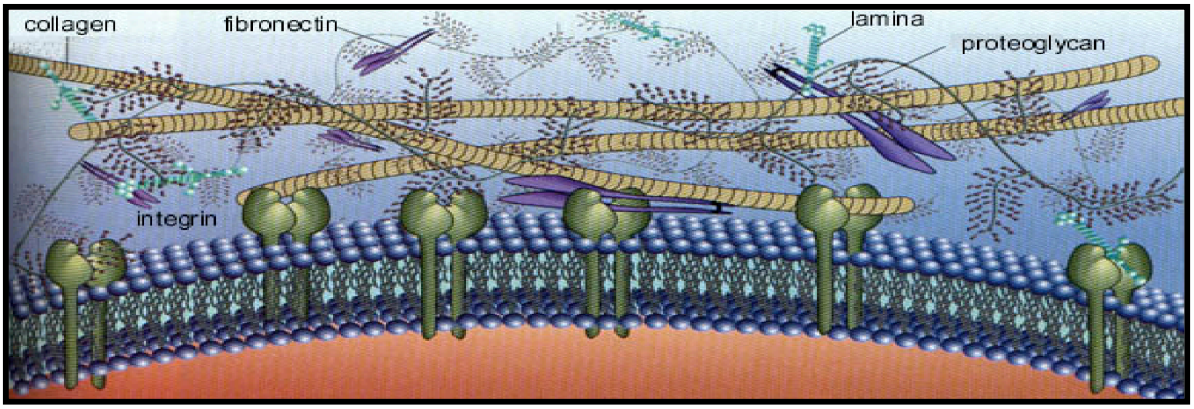

Fig. 2.1 Extracellular matrix
(intranet.biolchem.ucla.edu/cm267a/iruelaarispe/200...)

Collagens are the most abundant proteins constituting the ECM. In addition to being responsible for the strength and shape of tissues, each collagen type has specific

sequence providing them with special features such as flexibility and the ability to interact with other matrix molecules and cells.

Proteoclycans are another large group of matrix molecules. Proteoglycans and glycosaminoglycans (GAGs) perform numerous vital functions during cell growth, adhesion, tissue resilience and filtering. Some proteoglycans have the capacity to bind other matrix molecules and growth factors, while others act as matrix receptors on the cell surface.

Through additional families of adhesion molecules, the fibronectins and laminins, the matrix components are linked to one another and to adjacent cells. Also members of these families perform important functions in regulating cell behaviour.

The major cell surface receptors that are responsible for the ECM-cell interactions are the integrins. They are transmembrane proteins consisting of two subunits (α and ß), which bind to collagen, fibronectin and laminin. Among several putative integrin-binding sites, the first one identified and best characterized is the RGD sequence (Arg-Gly-Asp), which is recognized by several members of integrin family. In addition to attaching cells to the ECM, the integrins serve as anchors for the cytoskeleton and the resulting interaction of the cytoskeleton and the ECM is responsible for the stability.

2.1.1 Extracellular matrix in periodontal tissues

The periodontium comprises the tissues that surround and support the teeth. It consists of gingiva, periodontal ligament (PDL) and alveolar bone (Fig. 2.2). The main functions of the periodontium are to support the teeth, to absorb the forces created by mastication and orthodontic movements and to protect teeth against constant attack by oral microorganisms (Uitto and Larjava, 1991). These functions are accomplished by an unusual high turnover rate of the periodontal tissue compared to virtually all other connective tissues (Sodek and Ferrier, 1988).

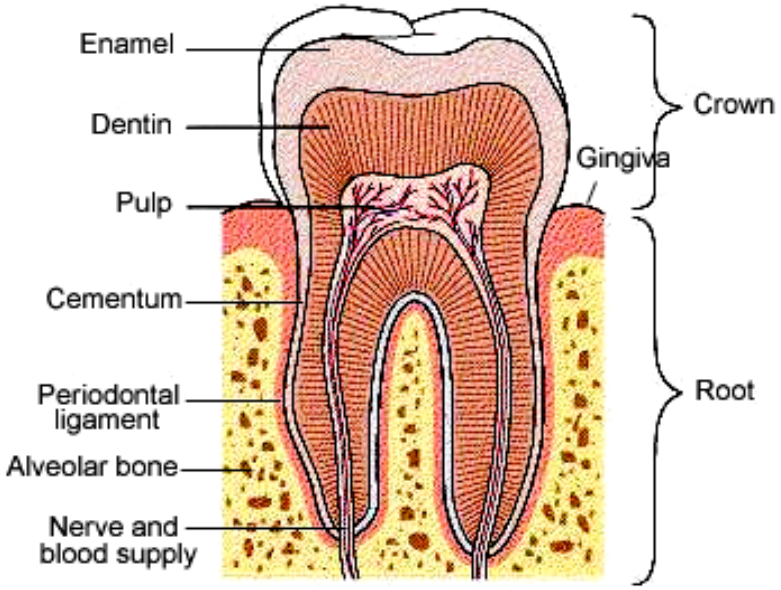

Fig. 2.2 The periodontium
The gingiva, periodontal ligament (PDL) and alveolar bone surround and support the teeth. The tooth is anchored to the surrounding alveolar bone by the PDL. The PDL is a specialized fibrous connective tissue that contains blood vessels and nerves situated between collagen bundles of the PDL and it acts as a sensor for the uptake of the forces created by the orthodontic movements and mastication. (117DentalMatls031406).

The main structural cell type of subepithelial gingiva and PDL tissues is the fibroblast. The PDL is a dense connective tissue, formed primarily of thick collagen fiber bundles that are functionally oriented to attach and support the teeth.

The ECM underneath the gingival epithelium forms a basement membrane (BM). On the ultrastructural level, this BM can be divided into the lamina lucida, containing laminin and lamina densa, which consist of collagen type-IV (Tomakidi et al., 1997). During development, the BM components, laminin and collagen IV, support the dental epithelium. However, in the late stage of development, when the processes of

enamel matrix secretion and calcification have begun, the BM structure between the dental epithelium and the mesenchyme disappears.

In addition to non-fibrillar collagen type-IV, gingival tissue and PDL contain collagen type-I (Fujita et al., 2002). Collagen type-I together with collagen types-II, III, V and XI form the group of fibrillar collagens, whose main function is to provide mechanical strength to the tissues expressing them (Narayanan AS., 1985). Apart from proteoglycans, which are ubiquitous constituents of the periodontal tissues, fibronectin is also found in connective tissues of the periodontium including PDL and bone (Pitaru et al., 1987). The fibronectin gene encodes for various glycoprotein isoforms generated by alternative splicing, which promote cell adhesion, migration, differentiation and cytoskeletal organization. It has been demonstrated that fibronectin supports the proliferation and chemotaxis of PDL fibroblasts in vitro (Kapila et al., 1998). Moreover, PDL fibroblasts respond to the application of mechanical forces by significantly increasing their production of collagen type-I and fibronectin (Howard et al., 1998).

In alveolar bone and cementum specialized cells, osteoblasts and cementoblasts lay down the matrix, of which collagens make over 90% of its organic constituents.

Fibroblasts in the gingival connective tissue and PDL, osteoblasts and gingival keratinocytes express integrin receptors, which bind to fibronectin with various affinities (Smith et al., 1990). Interference with the cell-matrix interactions can result in degradation of the subepithelial basement membrane that might lead to periodontal diseases. Cell-matrix interactions also have a central role in the healing of periodontal tissue following therapy.

2.2 Periostin – a fasciclin-like extracellular matrix protein

Proteins containing fasciclin domains have been shown to function as adhesion molecules (Elkins et al., 1990; Kawamoto et al., 1998; Kim et al., 2000). Fasciclin- like family proteins contain variable number of fasciclin domains and were first identified in insects (Bastiani et al., 1987). Over the past years, proteins containing fasciclin domains have been found in algae (Algal-CAM) (Huber and Sumper, 1994), bacteria (MPB70) (Ulstrup et al., 1995), Drosophila (midline fasciclin) (Hu et al., 1998) (Elkins et al., 1990), mouse and humans (ßig-h3, periostin, stablin I and II) (LeBaron et al., 1995; Takeshita, 1993).

Periostin (OSF-2) is a fasciclin domain containing protein, which was originally identified using a subtraction hybridization and differential screening approach from a mouse osteoblastic MC3T3-E1 cDNA library **(**Takeshita**,** 1993**)**. Western blot and immunohistochemical analysis showed that periostin is a 90 kDa secreted N-glycosylated protein present in the ECM.
The amino acid sequence of periostin has homology regions with Fasciclin I, a protein expressed on the surface of a subset of axon pathways in the embryonic central nervous system of insects (Zinn et al., 1988). In 1992, Skonier et al. identified a protein with a relatively high homology to periostin, ßig-h3, previously known as the 68 kDa transforming growth factor (TGF)-ß1-inducible protein that promotes adhesion and spreading of fibroblasts in vitro (LeBaron et al., 1995).

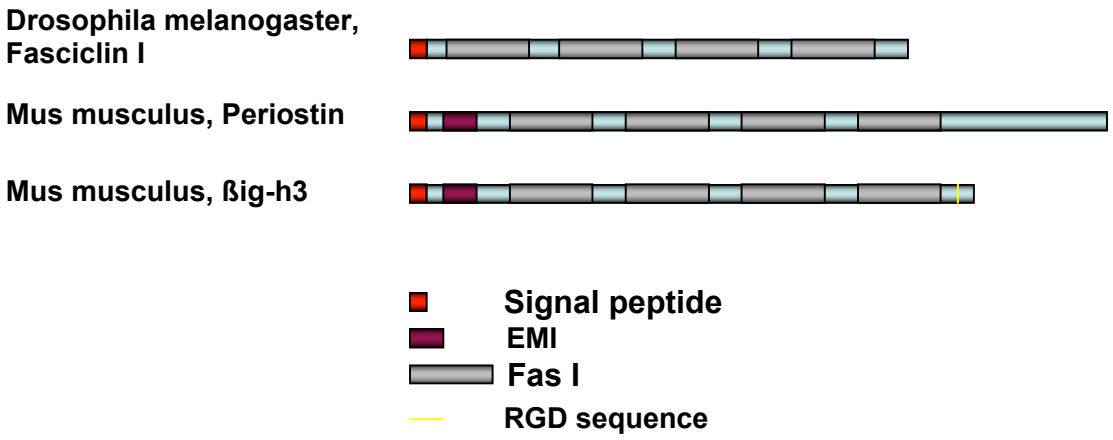

Fig. 2.3 Schematic presentation of Fasciclin I-like family proteins; Periostin and ßig-h3

The originally identified murine periostin is composed of 811 amino acids and contains four repeats of the fascilin domains, each of approximately 150 amino acids. All fasciclin domains contain two highly conserved regions (H1; H2) of approximately 10 amino acids each (Kawamoto et al., 1998). A cysteine-rich EMI domain is found at the N terminus following the signal peptide. This domain is found in proteins that form multimers (Doliana et al., 2000). Some authors also identified a putative nuclear localization signal at the carboxy-terminus. The periostin mRNA is alternatively spliced and the isoforms differ in the C-terminus of the protein. Recently, a periostin isoform was identified referred as periostin-like factor (PLF) that differs in the C-terminal region between amino acids 673 and 699 (Litvin et al., 2004). The difference between Periostin and PLF is in their temporal and tissue- specific expression pattern thereby indicating a functional difference between two isoforms (Litvin et al., 2006).

A highly homologous protein of periostin is ßig-h3. This 68kDa secreted protein (Ferguson et al., 2003; Park et al., 2004) is composed of 683 amino acids and contains four highly conserved fasciclin domains. Each fasciclin domain comprises 140 amino acids. Its signal sequence is followed by an EMI domain at the N-terminus and RGD sequence (Arg-Gly-Asp) at the C-terminus (Skonier et al., 1992). ßig-h3 is able to form fibrillar structures and strongly interacts with other ECM proteins, such as type I collagen, laminin and fibronectin (Nam et al., 2003; Ohno et al., 2002). In cell culture experiments it was shown that ßig-h3 is involved in cell spreading, adhesion, proliferation and migration (Bae et al., 2002; Billings et al., 2000; Ferguson et al., 2003; Jeong and Kim, 2004; Kim et al., 2003; Kim et al., 2000; LeBaron et al., 1995). These functions are mediated through interactions between the Fas domains and integrin receptors, such as $\alpha_3ß_1$, $\alpha_vß_5$, $\alpha_vß_3$ and $\alpha_6ß_4$ (Bae et al., 2002; Nam et al., 2003; Park et al 2004; Jeong and Kim, 2004).

In recent years, different functions have been proposed for the periostin protein based on the expression data and cell culture experiments. It was suggested that periostin might be involved in regulating adhesion and differentiation of osteoblasts and that it might play a role in response to mechanical forces of the tooth (Horiuchi et al., 1999). In recent studies, the high expression level of periostin in developing and mature heart valves (Kruzynska-Frejtag et al., 2001; Norris et al., 2004) and in developing teeth as well as the mature PDL (Kruzynska-Frejtag et al., 2004) was described. Expression in the ECM of the periosteum and the PDL in the adult mouse suggests that periostin might be involved in regulating adhesion and differentiation of osteoblasts and that it might also play a role in responses to mechanical forces on the teeth (Horiuchi et al., 1999). Additionally, it was shown that periostin regulates adhesion and migration of ovarian epithelial cells via its binding to the $\alpha_vß_3$ and $\alpha_vß_5$ integrins (Gillan et al., 2002; Yoshioka et al., 2002). Periostin expression was also detected in smooth muscle cells, in the neointima and adventitia and the protein was associated with smooth muscle cell differentiation and migration in vitro (Lindner et al., 2005).

A significant increase in periostin expression was observed in rat carotid arteries after balloon injury (Lindner et al., 2005) as well as in arterial smooth muscle cells in response to the stress of hypoxia. This was mediated through the P13K/p70Sk6, Ras/MEK1/2 and Ras/p38MAPK signalling pathways (Li et al., 2005). These findings suggested that periostin might play an important role in adult tissues under conditions such as damage and stress.

Significantly reduced levels of periostin mRNA were recorded in many human cancer cell lines and tissues. When periostin levels were increased by infection with recombinant retrovirus containing C-terminal region of the periostin protein, some cancer cell lines displayed a reduced growth (Yoshioka et al., 2002).

In the first approach to unravel periostin functions in an organism, Morpholino antisense experiments were performed in the Zebrafish. The treatment affected the structures of sarcolemmas and myofilaments and the motility of the zebrafish embryos, thereby demonstrating the importance of periostin for the adhesion of the muscle fibers to the myosepta and for the differentiation of muscle fibers (Kudo et al., 2004).

2.3 Tooth development

2.3.1 Dentition in human and mice

The mouse has in each quadrant three molars at the back of the mouth, which are separated from the incisors at the front by a toothless region called diastema (Fig. 2.4) (Tucker and Sharpe, 2004). Many rodents, including the mouse, have rudimentary tooth germs in the diastema region (Peterkova, 1985), which are believed to be remnants of the primitive dental incisors, a canine, premolars and molars (Luckett and Maier, 1982; Peterkova, 1985). It has been shown that mouse tooth germs in the diastema region degenerate at the early bud stage (see below) (Keranen et al., 1999).

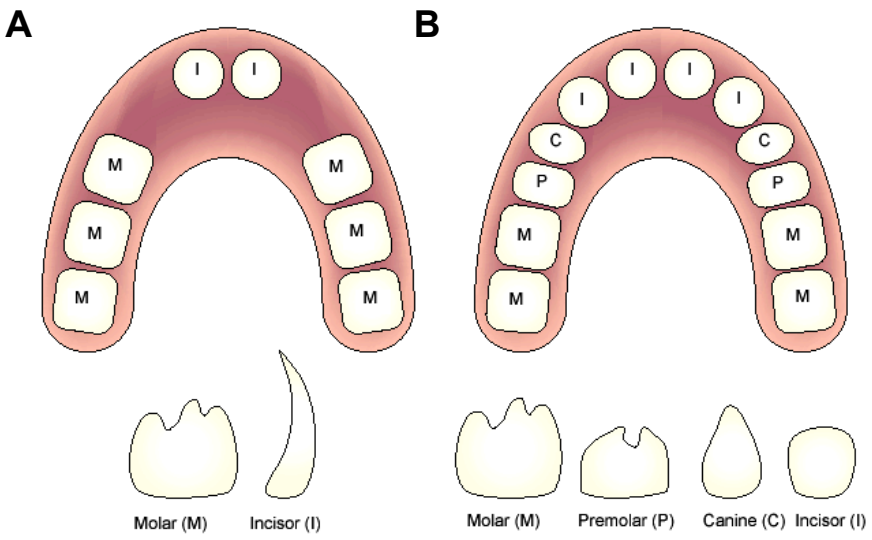

Fig. 2.4 A comparison of mouse and human dentition
Mouse dentition contains one incisor and three molars in each quadrant that are separated by a toothless region, diastema (A). The primary or deciduous human dentition, which is presented here consists of two incisors, a canine, a premolar and two molars developing in each quadrant (B) (Tucker and Sharpe, 2004).

Humans have extra tooth types in comparison to mouse. Human dentition consists of canines and premolars, which are formed by processes similar to tooth development in mouse but with higher levels of patterning complexity (Tucker and Sharpe, 2004).

2.3.2 Overview of tooth development

Mammalian organs comprise epithelial and mesenchymal tissues. During development, sequential and reciprocal interactions between these tissues regulate the formation of different organs by inducing morphogenesis and cellular differentiation (Kollar and Lumsden, 1979; Thesleff and Aberg, 1997; Thesleff and Hurmerinta, 1981). At the molecular level, these interactions are mediated by signalling molecules, their receptors, transcription factors and cell adhesion molecules (Wang et al., 2004). Teeth are one example of an organ whose early development is characterized by epithelial-mesenchymal interactions. For a long time, these processes have been studied in order to get more answers on the nature of epithelial-mesenchymal interactions and the molecular regulation of organogenesis.
All teeth, regardless of shape or identity, pass through the same developmental stages, and consist of the same tissues (Butler, 1995; Stock et al., 1997). The odontogenic potential, which originates from the oral epithelium, is transferred into the underlying neural crest derived mesenchyme, and mesenchymal signals are necessary for further epithelial morphogenesis and cytodifferentiation.

Tooth development has been divided into three partially overlapping phases of initiation, morphogenesis and cell differentiation (Kollar and Lumsden, 1979) (Fig. 2.5). During tooth initiation, the oral epithelium thickens (dental lamina) and grows into the mesenchyme in the shape of a bud (bud stage). The epithelium signals to

the mesenchyme and proliferating mesenchymal cells surround and condense around the epithelial bud.

During subsequent morphogenesis, the epithelium (enamel organ) folds and grows to surround the dental papilla mesenchyme (cap stage) (Fig.2.5). Cells adjacent to the dental papilla and those that lie outside the enamel organ divide and grow around the enamel organ to form the dental follicle or dental sac. These three structures constitute the tooth germ and give rise to the tooth and its supporting structures. At this stage, a cluster of condensed cells can be seen above the dental papilla mesenchyme, constituting a transient signalling center, the primary enamel knot. The enamel knot soon degenerates by apoptosis.

The enamel organ and adjacent dental papilla increase further in size in the bell or differentiation stage (Fig. 2.5). At late bell stage, the inner enamel epithelial cells elongate and differentiate into ameloblasts, the future enamel-forming cells. The cells of the dental papilla differentiate into odontoblasts. As they differentiate, they elongate and secrete the dentin matrix.

The center of the enlarged enamel organ, the stellate reticulum, is formed by large, star-shaped cells containing many branching processes. Between the stellate reticulum and inner dental epithelium are two or three layers of flattened cells forming the stratum intermedium. The secondary enamel knots start to form at the tips of the future cusps governing the folding of the dental epithelium and determining the shape of the tooth crown (Jernvall and Thesleff, 2000).

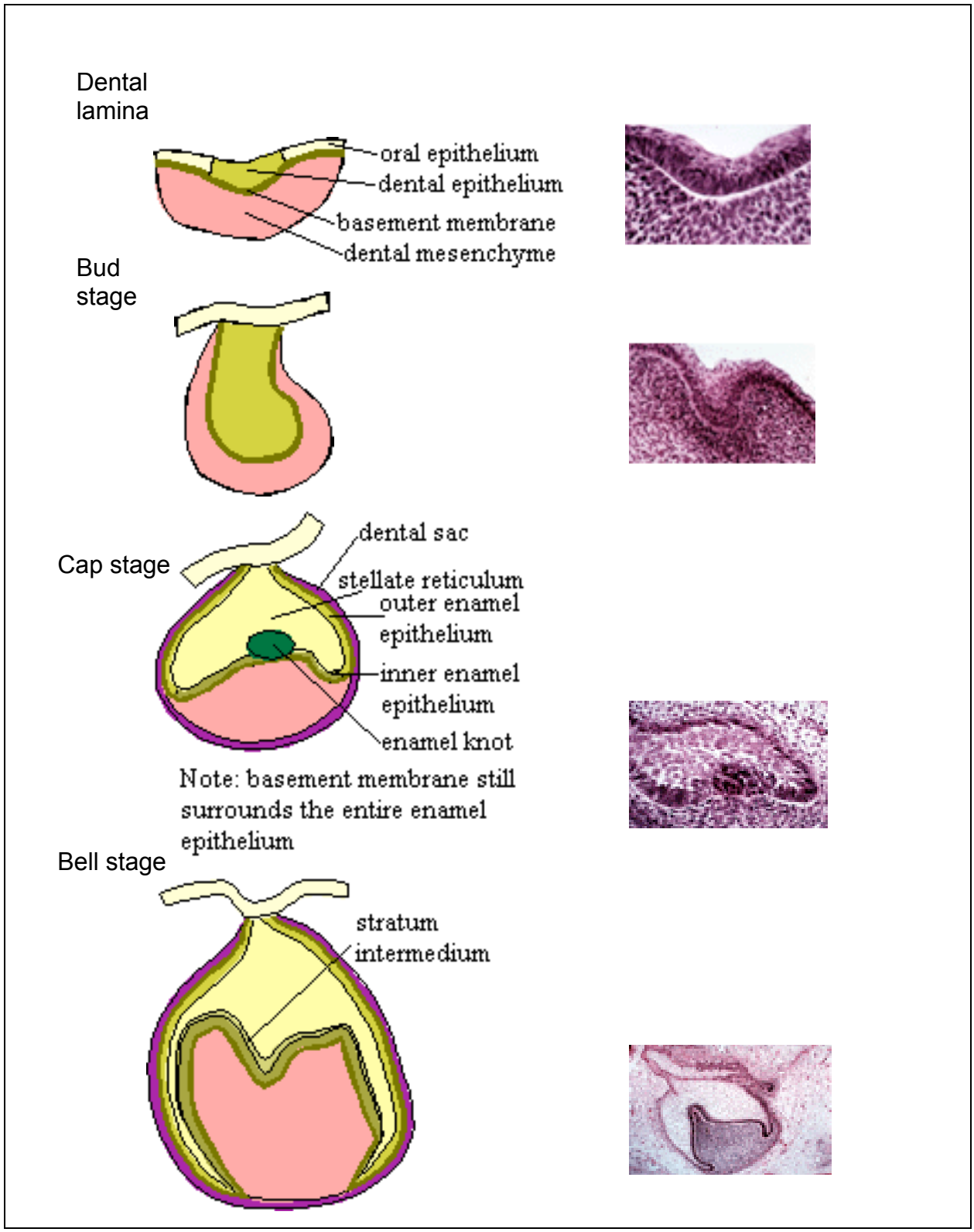

Fig. 2.5 Schematic overview of molar tooth development
(The Gene Expression in Tooth site of the University of Helsinki; Oral Histology)

The final cell differentiation occurs during the bell stage of tooth development.
The cells of mesenchymal origin underlining the epithelium become postmitotic, polarize and start to secrete predentin, the organic matrix of dentin. Initially they are called preodontoblasts and are organized in a single layer at the periphery of the dental papilla. As differentiation proceeds, these cells elongate and polarize. They have an increased number of organelles. While synthesizing the dentin matrix, the odontoblasts form long cell processes, which are embedded in the dentin matrix (Ruch, 1987). The dentin matrix proteins consist of type I collagen and some non-collagenous proteins (proteoglycans, glycoproteins and dentin sialophosphoprotein (MacDougall et al., 1998).
The process of amelogenesis is a series of successive stages of ameloblast cell proliferation, differentiation, secretion and maturation (Smith, 1998). Ameloblasts arise from the inner enamel epithelial cells (preameloblasts). The cells of the epithelium become post-mitotic shortly after the mesenchymal cells, but they polarize only after a layer of predentin has been secreted by the odontoblasts (Ruch et al., 1972).
Tooth development is strictly genetically regulated. Many genes that have been identified to regulate embryonic development in other organs are linked with tooth morphogenesis as well. They include several members of secreted signalling molecules such as the hedgehogs, fibroblast growth factors (FGF), Wnt and TGF-ß (transforming growth factor ß) families. Through the interactions with specific cell surface receptors they regulate the expression of genes which will finally determine the identity, size, location and shape of the teeth (Thesleff, 2000).

2.3.3 Amelogenesis

Amelogenesis or enamel formation occurs in several successive stages. These include a) presecretory, b) secretory, c) transition, d) maturation, e) post-maturation or protective stages.

Differentiation of the inner dental epithelium into pre-ameloblasts begins during presecretory stage. Pre-ameloblasts are cubiodal cells with centrally oriented nuclei, which induce dental papilla cells to differentiate into odontoblast. Odontoblasts form dentin. Once the certain amount of dentin matrix is formed by odontoblasts, pre-ameloblasts start to differentiate into ameloblasts and secrete enamel matrix.

Secretory ameloblasts, like odontoblasts, are polarized cells with a secretory (Tomes′ process) or apical end and non-secretory basal end (Fig. 2.6). Intracellular changes involve a lengthening of the cell, proliferation of the endoplastic reticulum (ER), and redistribution of cellular organelles (basal migration of the nucleus and apical migration of the Golgi apparatus-repolarization (Avery J.K. 2001).

Ameloblasts secrete several classes of matrix proteins (amelogenin, ameloblastin, enamelin, tuftelin, laminin 5, dentin sialophosphoprotein) and later proteolytic enzymes (metalloprotease and serine protease) for degradation of matrix proteins during maturation stage of enamel formation (Robinson et al., 1998; Robinson et al., 1995).

When the full thickness of enamel is achieved, ameloblasts secretion terminates and ameloblasts enter the post secretory or the transition stage when they loose their secretory elements (Tomes′ process). They become shorter and many (up to 50%) of the ameloblasts die by apoptosis. Following these changes, enamel maturation or mineralization begins. At this stage, protein degradation and removal of the proteinaceous remnants and water from the enamel matrix occurs. Consequently, the mineral content increases.

The smallest repeating unit of the enamel mineral phase is calcium hydroxyapatite [$Ca_{10}(PO_4)_6(OH)_2$]. These initial crystals are organized spatially into rod and interrod regions as they form, and rod crystals are lengthened by Tomes′ processes with

appositional movement of ameloblasts away from the dentin surface. Loss of protein from the matrix and a gain in mineral is easily visualized in decalcified histological sections.

In addition to their fundamental role in enamel formation, at the maturation stage, ameloblasts incorporate iron and deposit it onto the surface of the mature enamel, thereby causing a brownish yellow colour of the rodent incisors (Halse, 1973; Halse, 1974; Halse and Selvig, 1974; Kallenbach, 1970). It was shown that there also exist secretory cells capable of enamel-like matrix secretion (including amelogenin, ameloblastin…), but these cells do not have Tome′s processess like the ameloblasts (Bosshardt and Nanci, 1998; Sakakura et al., 1989).

The short, remaining ameloblasts together with the outer dental epithelium form protective layers (protective stage) on the enamel until the eruption of the tooth into oral cavity (Smith, 1998). Because these residual ameloblasts are lost when the tooth erupts, enamel cannot be repaired later in life.

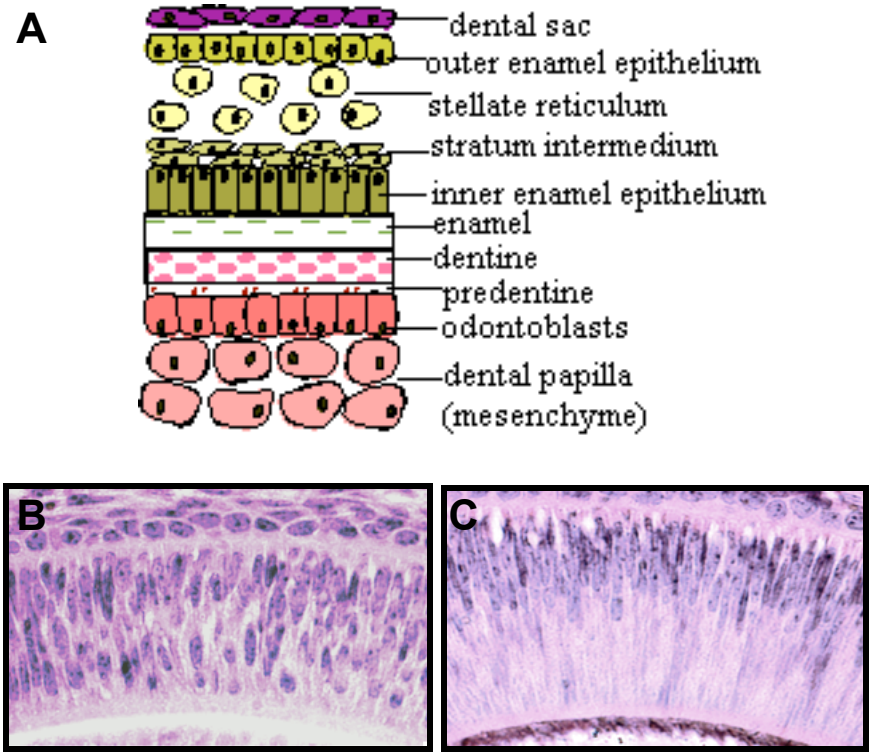

Fig. 2.6 Ameloblasts differentiation
Secretory stage (A); Preameloblasts are derived from precursor cells in the inner dental epithelium of the enamel organ (B). Upon differentiation, their size increases dramatically with extensive development and redistribution of cytoplasmic organelles (Ten Cate, 1998). Secretory ameloblasts are highly columnar and polarized with oval-shaped nuclei located at their non-secretory end (C) (The Gene Expression in Tooth site of the University of Helsinki).

In the molars, cell differentiation starts at the area of cuspal tips and proceeds in a cervical direction. There are some enamel-free areas on the occlusal surface of the molar crowns. In contrast to the multi-cuspid molars, incisors are mono-cuspid teeth. In rodent incisors, enamel is only formed on the labial side of the incisors, whereas the lingual surface is enamel-free and covered by cementum. Odontoblasts and dentin matrix are distributed on both sides of the incisors (Fig. 2.7).

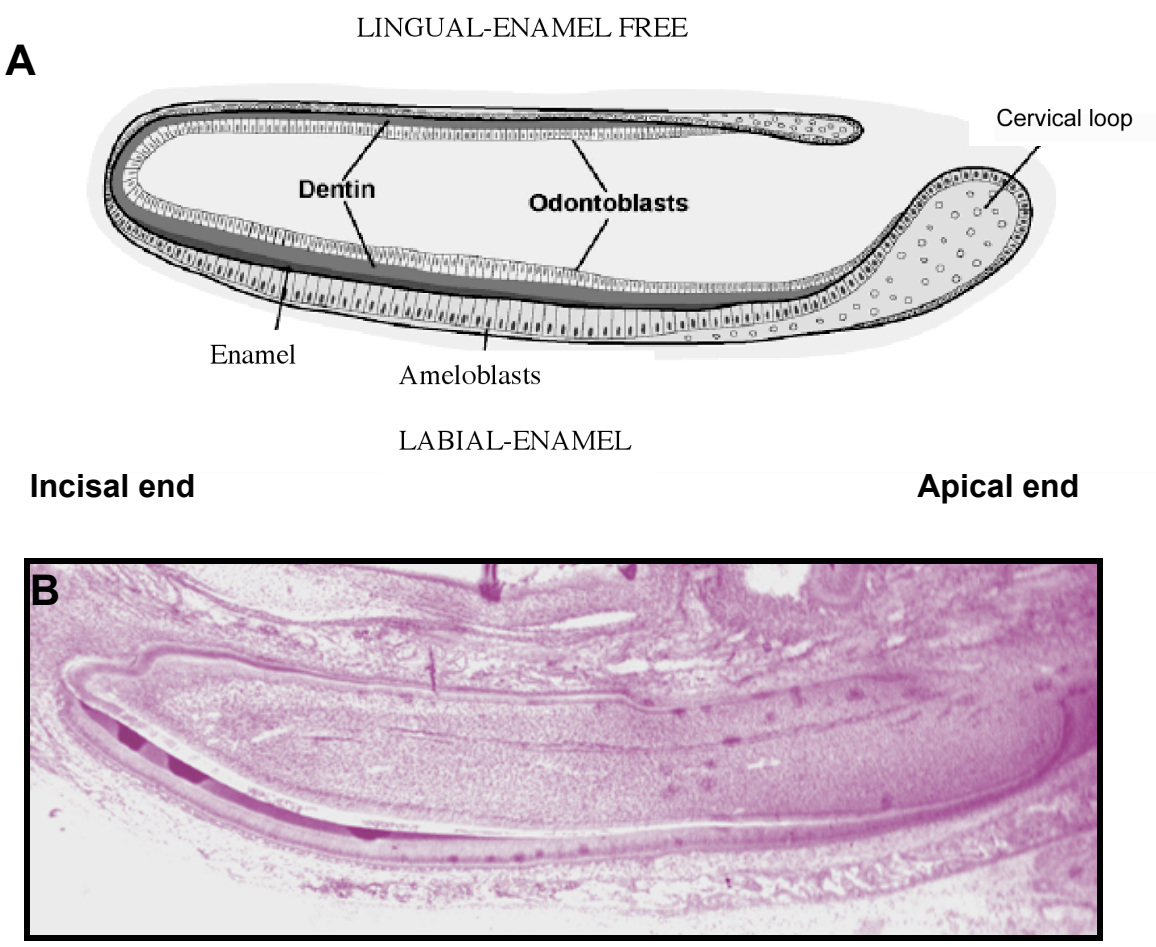

Fig. 2.7 Mouse incisor development
Cytodifferentiation begins at the late bell stage when epithelial cells on the labial side of the incisor differentiate into ameloblasts, which secrete the enamel matrix.
The stem cells in the cervical loop region support the continuous growth of rodent incisors.
(A, Xiu-Ping Wang, Disssertation 2004, Helsinki; B, Wiild type mandibular incisor at P3, H&E).

A characteristic feature of rodent incisors is their continuous eruption throughout life implicating the presence of stem cells in the cervical loops at the base of the tooth (Harada et al., 1999; Harada et al., 2002; Smith and Warshawsky, 1975). In sagittal sections, all development stages from the undifferentiated precursors at the apical end to the fully differentiated cells at the incisal end can be observed (Fig. 2.7).

For the ameloblasts, these stages from the apical end toward the incisal end are classified regionally into presecretory, secretory, transition and maturation stages.

2.4 Tooth eruption

Tooth eruption is defined as the movement of a tooth from its site of development within the alveolar process to its functional position in the oral cavity (Massler, 1941). Teeth develop in the alveolar bone. During crown formation there are small preeruptive movements within the jaws. After crown formation is completed and the root begins to form, an active eruption process moves the tooth towards its functional position.

In the past, numerous theories of tooth eruption have been proposed, which involved almost all tissues in or near an erupting tooth. However, it was shown that none of the theories alone can account for all of the movements made by a tooth during its lifetime (Marks and Schroeder, 1996).

Focussing on teeth with limited eruption, it was thought that root growth and pulpal pressure were fundamental factors (Massler, 1941), until cases of eruption of rootless teeth, obtained by surgical excision of the growing root, were reported (Perl and Farman, 1977; Shields et al., 1973). Since surgical excision of the growing root and associated tissues eliminates the apical vasculature without stopping the eruption, this revealed that also the local vessels are not absolutely necessary for tooth eruption (Herzberg, 1941).

Another theory was that fibroblasts of the PDL move out and pull the teeth by the help of collagen bundles attached to the surface of the teeth. This theory was checked by the administration of lathyrogens. Lathyrogens are drugs that specifically inhibit the formation of collagen crosslinks. These experiments had no effect on the eruption of the teeth in the experimental animals (Sutton and Graze, 1985). Though an involvement of the fibroblasts of the PDL in the eruption process cannot be

excluded by these experiments, the numerous collagen bundles that were thought to be of great importance are obviously not absolutely required for eruption.

Osteopetrotic rodents have revealed the importance of alveolar bone resorption in tooth eruption. Osteopetrosis is a congenital bone disease characterized by reduced bone resorption but not reduced bone formation (Marks, 1973). In these animals, teeth are fully formed but cannot erupt because they are trapped inside the bone (Cotton, 1974). Probably non-functional or undernumbered osteoclasts caused this phenotype by the absence of bone resorption in the crypts of rats (Marks, 1973); (Marks, 1977; Seifert et al., 1988).

In several studies, a possible role of the adjacent dental follicle in the process of bone resorption and therewith in the eruption was examined (Cahill and Marks, 1980; Marks and Cahill, 1987; Marks et al., 1983). Originating from cranial neural crest mesenchyme, the dental follicle (DF) is a loose connective tissue, which surrounds the enamel organ. It is separated from the latter internally by a basement membrane and separated from the bone cells by a loose vascular connective tissue (Schroeder et al., 1992). It was shown that removal of the dental follicle in the dog premolars prior to the onset of eruption prevented the unerupted teeth from erupting (Cahill and Marks, 1980). A later study revealed that the polarized resorption and formation of alveolar bone that occur around a tooth during eruption are regulated by the dental follicle (Cahill and Marks, 1980; Marks and Cahill, 1987; Marks et al., 1983). Therefore, dental follicle, bone resorption and formation are required for the eruption to occur (Wise et al., 2002).

Periodontal ligament and tooth eruption

The derivative of the dental follicle, the PDL, appears to play a role in continuous eruption of rodent incisors (Berkovitz, 1971; Berkovitz and Thomas, 1969). The PDL is the soft connective tissue interposed between cementum of the teeth and the inner wall of the alveolar bone. It links the teeth to the alveolar bone, providing support, protection and provision of the sensory input to the masticatory system (Beertsen et al., 1997).

The periodontal ligament contains several cell types. Fibroblasts, which (in rodent molars) occupy about 35% of the volume of the periodontal ligament space (blood vessels excluded) are predominant (Beertsen, 1975). The cells covering the surface of both cementum and alveolar bone (cementoblasts and osteoblasts) are considered part of the ligament and have a similar mesenchymal origin. In addition, the periodontal ligament contains undifferentiated mesenchymal cells, defence cells and aggregations of epithelial cells. These are remains of the epithelial root sheaths and are called rests of Malassez (Fig 2.8).

The major fibers of the ligament are mainly collagenous, but there are also small amounts of oxytalan and reticulin fibers and, in some species, elastin fibers. The main types of collagen found in the periodontal ligament are types I and III. Small amounts of types V and VI have been detected as well as traces of basement membrane collagens associated with epithelial cells and blood vessels. The collagen forms bundles that are termed the principal fibers. The principal fibers of the periodontal ligament that are embedded in the cementum and in the bone lining the tooth socket are termed Sharpey′ s fibers.

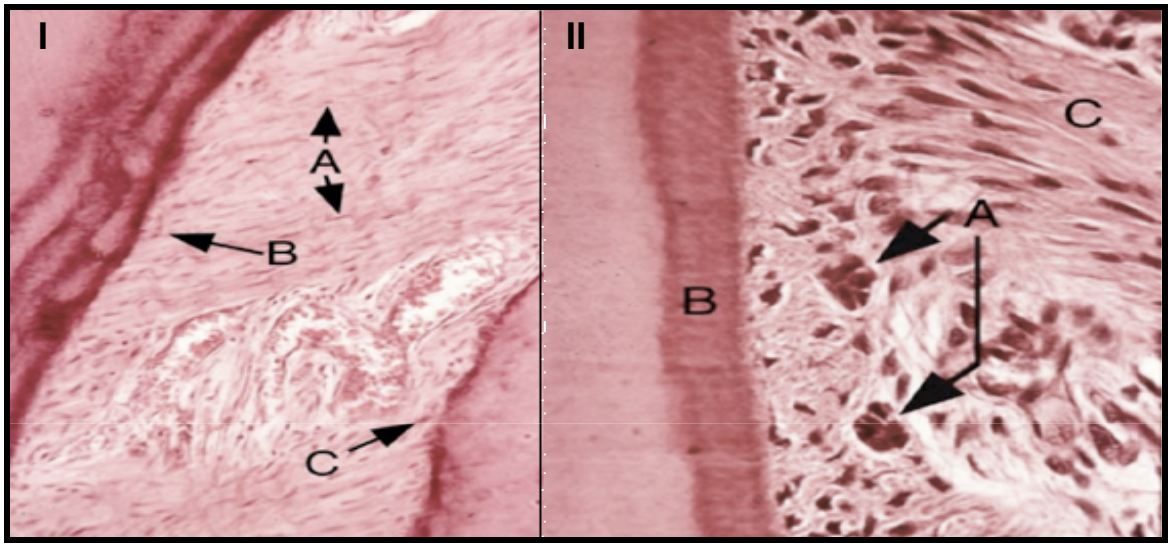

Fig. 2.8 Periodontal ligament
The main cell type in the periodontal ligament is the fibroblast. Adjacent to the cementum are cementoblasts, and adjacent to the bone are osteoblasts; **I** (**A**, fibroblasts; **B**, cementoblasts; **C**, osteoblasts); Remnants of the epithelial root sheath that remain following its disintegration during root formation are called epithelial rests; **II** (**A**, Epithelial rests; **B**, Cementum; **C**, Periodontal ligament) (Oral Histology).

The PDL of a tooth of limited growth shows, at one stage in its development, the presence of three zones of fibers: (1) alveolar fibers, which are attached to the alveolar bone; (2) cemental fibers that are connected to the surface of the root; and (3) the intermediate plexus where alveolar and cemental fibers meet, intermingle and are interconnected (Orban, B., 1927). After the end of this period of rapid eruption, these separate zones are no longer visible (Eccles, J.D., 1959).

Similar zones are present during the development of the periodontal ligament in teeth of continuous growth (Eccles, 1965), but these remain clearly distinguished during the life of the tooth. Other authors discriminate two compartments in the PDL: one related to tooth (TRC) and the other adjacent to the alveolar bone (AC) (Beertsen et al., 1974). It has been suggested that the ligament in the TRC moves along with the incisor in the direction of the oral cavity while the ligament in the AC

compartment remains stationary (Beertsen, 1975). Between these two morphologically distinct regions a narrow so called „tissue shear“ zone can be found (Beertsen, 1973). Synthesis and turnover of total proteins occurs throughout the PDL, but the density of collagen containing vacuoles was demonstrated to be highest in the mid-region of the PDL by Beertsen and Everts (Beertsen and Everts, 1977). It has been proposed that this is the site of periodontal ligament remodelling during incisor eruption.

Periodontal ligament and alveolar bone are exposed to physical forces in vivo in response to mastication and orthodontic tooth movement. It is known that these processes as well as tooth eruption involve a remodelling of the periodontal and gingival connective tissue (Ten Cate et al., 1976).

All these data suggest that the PDL is important for tooth movements, however, for the molar teeth, which are characterized by a limited growth, the presence of the PDL alone does not assure eruption. In human mutations severely affecting the PDL, like dentinal dysplasia type I, eruption occurs suggesting that apart from the PDL other tissues contribute to the eruption process (Cahill and Marks, 1980; Marks and Cahill, 1987; Marks et al., 1983). It also has to be noted that in rodents, the PDL between the molars and the continuously erupting incisors might differ and there will certainly be discrepancies between rodents and man.

2.5 Aims of the study

The aim of study was to elucidate the biological function of the extracellular matrix protein, periostin, in vertebrates. To identify the roles of the periostin gene in vertebrate development, I have chosen a gene targeting approach in mice. Firstly, the generation of the periostin deficient mouse line will be described. The next parts describe a detailed analysis of the mutant animals. Surprisingly, mutant mice were viable, although approximately 25% of the mutants died shortly after birth for reasons that are still under investigation (unpublished results). Phenotypes of the surviving periostin mutants are described and discussed.

Chapter 3

Results

3.1 Generation of Periostin knockout mice

3.1.1 Construction of the targeting vector

The targeting vector was prepared using genomic DNA of the periostin locus, which was isolated from a library of 129/Ola mouse strain and the parental pTVFlox-O vector.

In general, the targeting vector consisted of two homologous genomic regions (5,6 kb "long arm" and 1,3 kb "short arm") both flanking the *LacZ* open reading frame, which was followed by a floxed neomycin cassette (*Neo*). A *herpes simplex virus-thymidine kinase* gene (*TK*) was placed downstream of the short arm (Fig. 3.2).

In detail, the genomic long arm was amplified by PCR using the following primers: 5′ -ACA GAG A**GC GGC CGC** AGA GG- 3′ and 5′- **TCG CGA** GCC ATC TTC AGC CC- 3′. This fragment contained 5´ regulatory sequences and the first exon up to the ATG. Subsequently, the *LacZ* open reading frame (ORF), a NruI-SalI fragment (isolated from pBluescript-LacZ vector) was ligated to the *periostin* 5,6 kb NotI-NruI fragment of the genomic long arm at the site of the start ATG of periostin´s first exon thereby fusing this ATG in frame to the *LacZ*-ORF (Fig. 3.1).

Downstream of the Neo cassette, a 1,3 kb genomic fragment (short arm) amplified by PCR was inserted as a SalI-AscI fragment 3´of the neo cassette and 5´of the TK cassette. This fragment contained intronic sequences and parts of the third exon. The following primers were used: 5′ -CCC CAG **GTC GAC** TTT TTC TGC- 3′ and 5′ -CCT GCG **GGC GCG CC**T TTC ATC CC- 3′.

*Lac Z .....**TCG**CGA*TGATCCC.....;

Periostin....GGGCTGAAG***ATG***GC**TCG**CGA**...;

Lac Z-Periostin fusion....GGGCTGAAG***ATG***GC**TCG**CGA*TGATCCC.....

Fig. 3.1 Periostin "long homolog arm" and *Lac Z* fusion

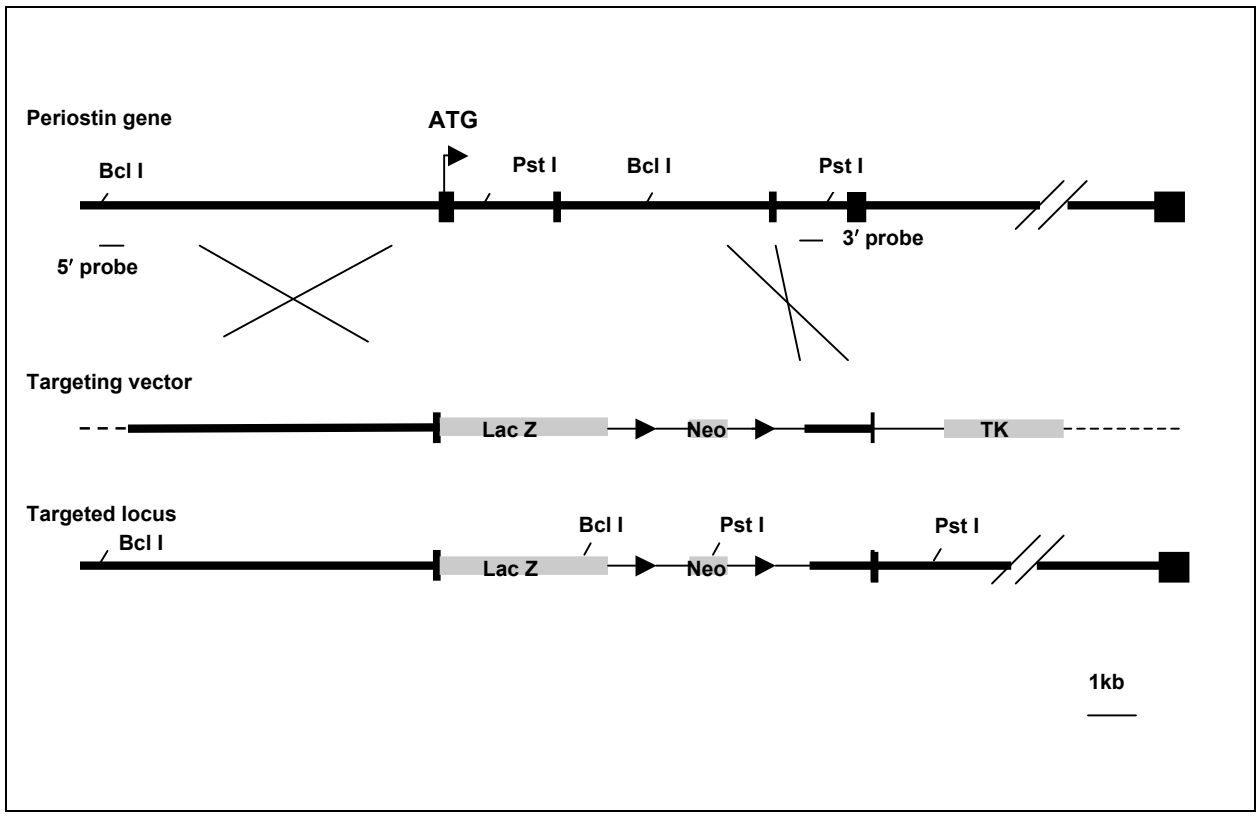

Fig. 3.2 Schematic representation of homologous recombination in murine embryonic stem cells (ES) cells at the periostin locus
The first four exons and the last exon of the periostin gene (top), targeting construct (middle) and the periostin locus after the homologous recombination event (bottom) are presented. The *Periostin-LacZ* substitution at the ATG start codon ensures *lacZ* gene expression under the control of endogenous periostin cis-regluatory elements. The *TK* cassette is outside the homologous regions, to select against random genomic insertion (Non-homologous-End-Joining). In order to confirm positive homologous recombination events, genomic DNA was digested with PstI and the indicated 3′ probe was used in a Southern Blot. To independently confirm homologous recombination at the 5′ end, genomic DNA was digested with BclI and the indicated 5′ probe was used in an additional Southern Blot.

3.1.2 Electroporation and selection of ES cells

Approximately, 25 μg of double-stranded linearized targeting-vector DNA was introduced into ES cells by electroporation. After seeding the electroporated cells and allowing them to grow for 24h in ES medium, selection was started by addition of the antibiotic Geneticin (G418). The neomycin gene confers resistance to G418

by enzymatic modification of the drug and is thus not lethal for ES cells expressing the gene. In order to distinguish between ES cells that had incorporated the targeting vector randomly into genome and those that had undergone homologous recombination at the periostin locus, negative selection was started four days after the electroporation by additon of Gancyclovir. The TK-gene enables cells to incorporate the drug into the DNA thereby interfering with replication. By this negative selection step the transfected ES cells were enriched for cells without an active TK gene.

3.1.3 Identification and verification of homologous recombination in ES cells and generation of the periostin-lacZ mouse

The ES cell clones that survived the selection, were isolated and individually expanded in 96well-plates. Expanded cells were split into two different plates. One plate was stored frozen while the other one was used for DNA isolation. Isolated genomic DNA was monitored for homologous recombination events by Southern blot analysis using the 561 bp 3′ external probe. By PstI digestion and hybridization with this probe a 5,2 kb wild type allele and a 2,9 kb targeted allele can be detected (Fig. 3.2). Two independent positive clones were identified from 1500 screened clones.
These positive clones were resurrected from the frozen plates and expanded. The homologous recombination event was confirmed again by Southern blot analysis using the same probe. To eliminate the possibility of multiple integrations of the targeting vector into the periostin locus, an additional Southern blot analysis was performed using the 452 bp 5′ external probe (Fig. 3.2). Following BclI digestion, hybridization with this probe identifies an 8,2 kb wild type allele and a 7,2 kb mutant allele.
These two independent ES cell clones were injected in C57/BL6 blastocysts and both gave rise to chimaeric animals that transmitted the mutant allel to their offspring. The corresponding mouse strain was named Periostin-LacZ while the

internal names for the independent clones are Per3B and Per3F. Animals were genotyped by PCR generating a 531 bp wild type band and a 775 bp „mutant“ band. Western Blot using adult dentin confirmed periostin deletion on the protein level.

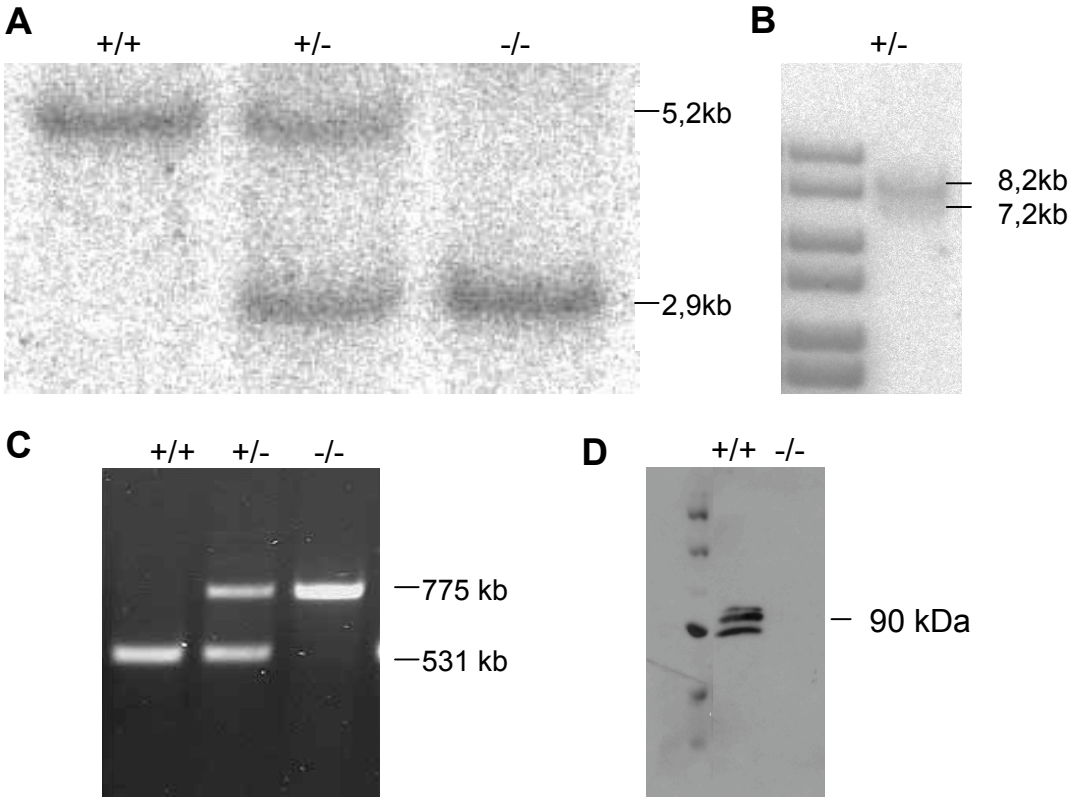

Fig. 3.3 Deletion of mouse Periostin
(A) Identification of homologous recombination by Southern blot analysis of genomic DNA. Genomic DNA was digested with PstI and hybridized with external 3′ probe. Homologous recombination additionally generates 2,9 kb „mutant“ band. (B) Southern blot analysis of genomic DNA, digested with BclI and hybridized with the 5′ external probe confirms the homologous recombination event by the presence of a „mutant“ 7,2 kb band. (C) Genotyping of Periostin deficient mice by PCR using genomic DNA, isolated from tailtips, by PCR that generates a 531 bp wild type and 775 bp „mutant“ fragment. (D) Complete absence of periostin was demonstrated by Western blot analysis in adult dentin.

3.1.4 Staining for LacZ activity

In order to ensure that the LacZ gene introduced into the periostin locus by homologous recombination is expressed in a periostin-like pattern, *LacZ* expression was analysed by monitoring enzymatic activity.

The bacterial ß-galactosidase enzyme encoded by the *lacZ* gene provides an easily detectable marker for expression using simple histochemical staining procedures. LacZ expression was detected within tissues and organs of the periostin heterozygous mice (Fig. 3.4). In general, periostin expression during embryonic development is higher than during postnatal development. ß-galactosidase activity could be detected as early as embryonic day (E) 9 (data not shown) in the developing heart. At E10 dorsal root ganglia (DRG), blood vessels, cartilage, liver, cranial mesenchyme and lungs showed strong β-galactosidase activity (Fig. 3.4A). The most abundant and strongest intensity of X-Gal staining was at E12 (Fig. 3.4B). From E14, the staining in expressing tissues and organs decreased while β-galactosidase activity in the skin persisted on a high level (data not shown). Lac Z expression could also be detected within tissue and organs of the adult heterozygous mice. Intensive blue staining is observable in skin, tissue surrounding the rips and bones (periosteum), and mandibles surrounding tissue (data not shown).

The Lac Z expression described here is in perfect accordance with data obtained by in-situ hybrization with periostin specific probes and immunohistochemistry using periostin specific antibodies (Michaela Miehe, Dissertation, Hamburg 2003 and unpublished data) demonstrating that ß-galactosidase expression recapitulates the endogenous periostin expression pattern.

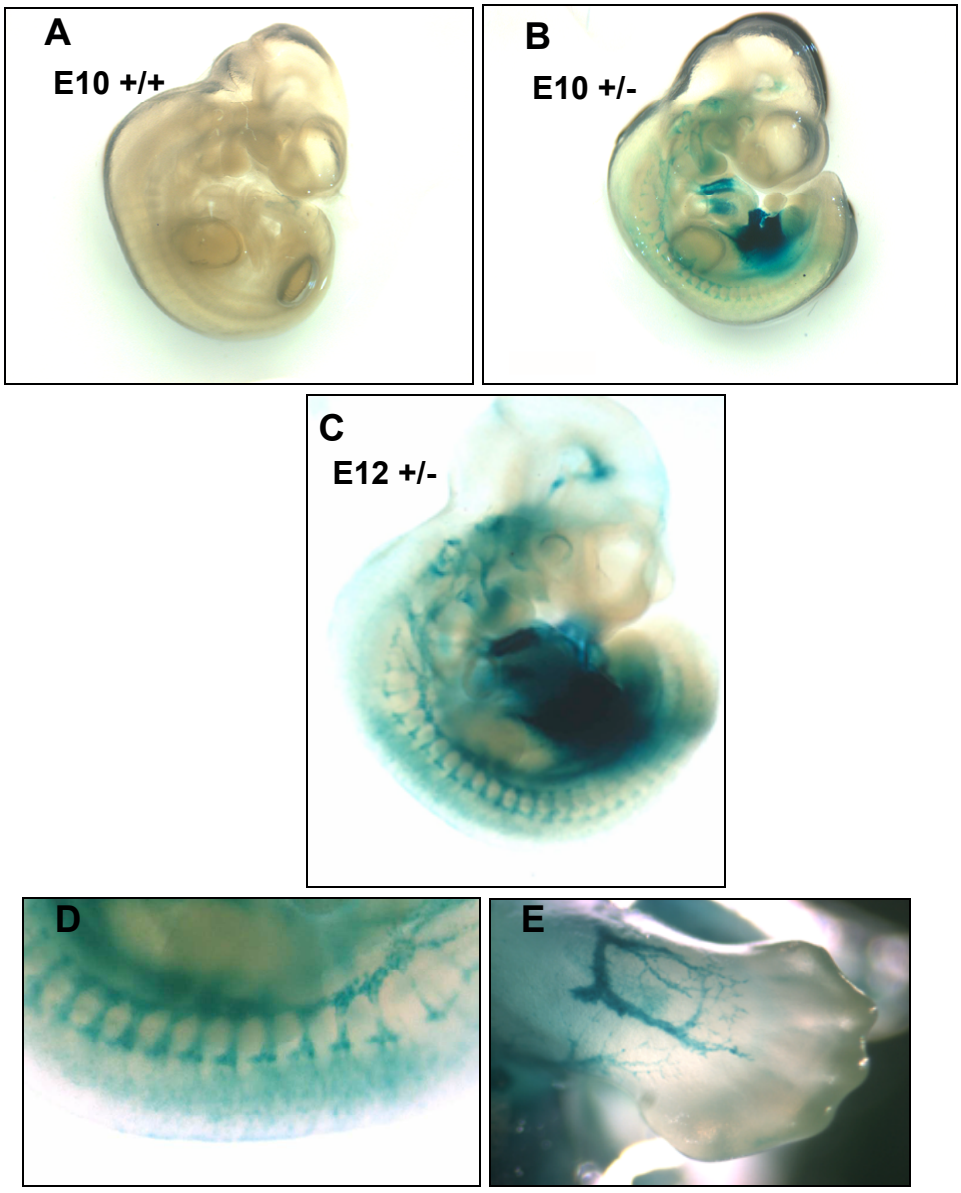

Fig. 3.4 Lac Z expression in periostin heterozygous embryos
The whole embryos were stained with X-Gal for half a day. (A, B) Heterozygous and wild type embryos from the same litter at E10. Note the strong expression in the heart and in the vessels passing into the umbilical cord. (C, D, E) Increased lacZ activity at E12 in a variety of tissues. Note the strong staining in ventral parts of the DRG (D) and blood vessels exemplified by the hindlimb (E).

3.2 Phenotypic characterization of Periostin deficient mice

3.2.1 Non-Mendelian ratio in offspring of heterozygous matings

Routinely, tailtips for genotyping were taken when the animals are separated from the mother at 3 weeks of age (post-weaning). The determination of genotypes at this stage revealed that animals carrying a null mutation of the periostin gene were reduced in number (17,5% instead of 25%), while no effect on sex specification could be observed (Fig. 3.5). However, statistical analysis of different embryonic stages showed, surprisingly, the expected Mendelian ratios (Fig. 3.6), which argued for a postnatal lethality. In order to further narrow down the time window of periostin deficiency induced lethality, genotypes were determined at P4 revealing that animals lacking Periostin had disappeared already at this stage. This indicated that the death of homozygous mutant animals that do not survive into adulthood occurs between P0 and P3.

According to the periostin expression pattern, a possible reason for the lethality originates from the expression in the developing heart. Periostin expression in the embryonic heart begins at E9 where it is detectable mainly in the endocardial cushions that later give rise to the valves of the heart. Expression is maintained in these structures during embryonic development and adulthood (data not shown) and (Kruzynska-Frejtag et al., 2001; Litvin et al., 2005).

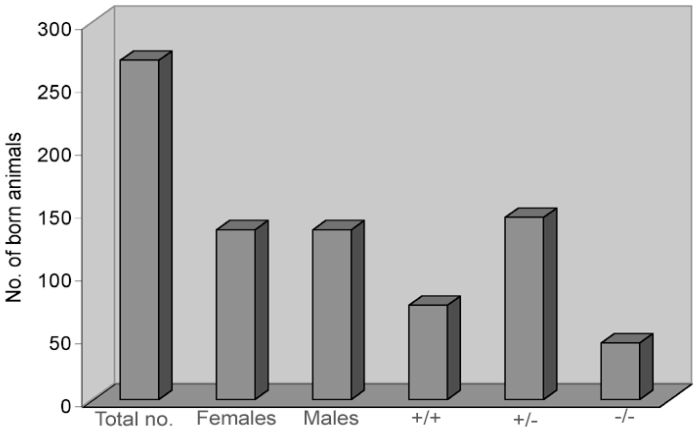

Fig. 3.5 Mortality of Periostin homozygous mutant mice
There is no significant difference in the number of born females and males. However, the number of surviving homozygous animals is around 25% lower than expected.

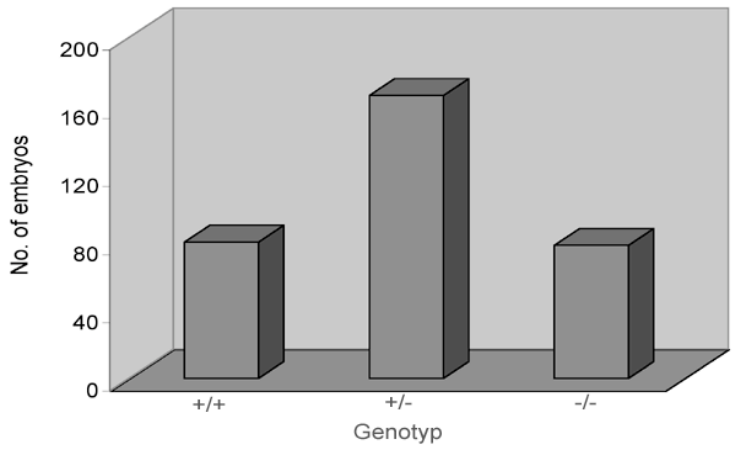

Fig. 3.6 Statistical analysis of genotypes during embryonic stages
Genotyping of embryos at different embryonic stages (E12- E18) revealed the expected number of living wild type, heterozygous and homozygous embryos. The graph represents the numbers of wild type, heterozygous and homozygous embryos from all embryonic stages.

Additional investigations are required to further clarify the defects that are causative for the observed lethality.

I made another interesting observation when homozygous animals were mated. Compared to other matings in that mouse strain (wt x heterozygous, heterozygous x heterozygous) the offspring rate as well as the littersize was dramatically reduced. I obtained only few litters (4) from homozygous matings and the litter size was only 3-4 compared to 8-12 in normal matings.

The reason for this reduced fertility requires further investigation. However, it cannot be excluded that nutrition deficits are causative or at least contribute to this phenotype (see chapter 3.2.2).

3.2.2 Decreased body weight and body size of Periostin deficient mice

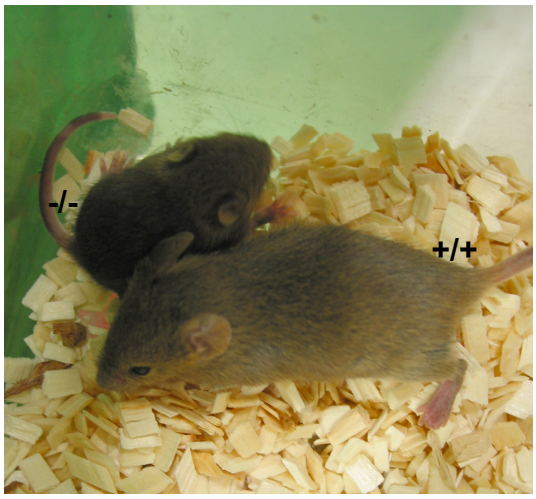

Fig. 3.7 Periostin deficient and wild type littermates at four weeks of age

Body weight and body size of the periostin deficient mice and their wild type littermates were largely indistinguishable during the first three weeks of life, after which the animals are weaned. Approximately one week later, most of the homozygous mutants, both females and males, showed reduced body weight compared to their wild type siblings of the same sex. A slight difference was observed between homozygous females and homozygous males, where homozygous males were even more affected than homozygous females (Fig. 3.8). Heterozygous animals did not reveal significant differences and show similar body weight and body size as wild type animals (data not shown).

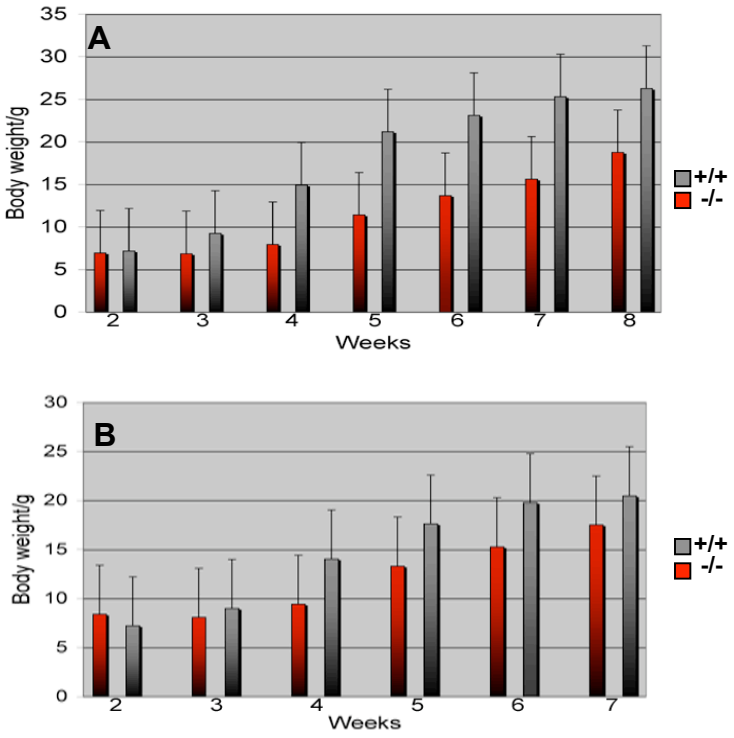

Fig. 3.8 Weight loss of periostin deficient mice
Each column represents the mean weight of mutant (red) and control (grey) animals (n=>8 e.g) at the indicated age for males (A) and females (B) kept on hard food (normal nutrition). Note that mutant males are more affected than females.

In order to further characterize these findings animals were kept in metabolic cages (data not shown). Metabolic cages (from Nalgene) are designed to allow for effortless separation of the urine and feces of mice. In addition, the specially designed feeding and drinking water bottle assemblies allow for the quantification of food and water that has been consumed for complete energy balance experiments. This experiment did not reveal significant differences between mutant and control animals demonstrating that the metabolism in mutant animals is normal. In the course of this experiment, animals were fed with powdered food and surprisingly mutant animals gained weight during the process of adaption to the metabolic cages.

Additionally, I observed defects in the appearance of the teeth (see 3.2.4). These two observations led me to examine whether the reduced body weight and size could be rescued by the application of soft food. Interestingly the weight was still slightly reduced in the first weeks after weaning (weeks 4-7). However, as can be seen in figure 3.9, mutant animals kept on soft food showed almost no reduction of body weight at postnatal weeks 8 and 9 (as well as therafter). This shows that the observed reduction in body weight and size of mutant animals under normal housing conditions (in particular with hard pelleted food) can be largely rescued by the application of soft food and thus is a secondary phenotype.

According to terms of animal welfare, periostin mutant animals were routinely kept on soft food except when indicated and scientifically necessary.

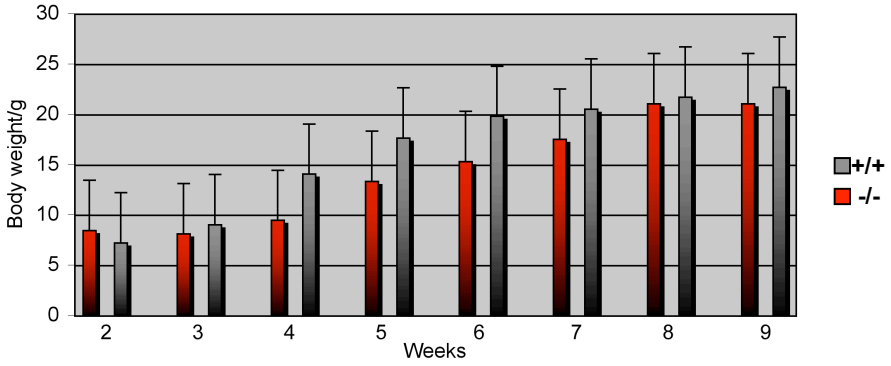

Fig. 3.9 Weight loss of periostin deficient mice can be largely rescued
Body weight of male and female homozygous animals and wild type controls (n=>8 e.g). The animals were kept on soft food and weight was measured once per week.

3.2.3 Comparable bone development of periostin deficient and control mice

Areas of highest periostin expression include periodontal ligament, the myotendinous junction and the periosteum of adult mouse femurs (Horiuchi et al., 1999; Wilde et al.,

2003; Doi et al., 2003; Kruzynska-Frejtag et al., 2001; Norris et al., 2004; Kern et al., 2005). Consistently, lacZ expression in the periostin lacZ strain revealed periostin expression in areas surrounding skeletal structures (cartilage and bone) and craniofacial regions (data not shown). Therefore, the structure of periostin deficient bone was examined.

Whole newborn (P0) and four days old (P4) control and periostin deficient mice skeletons were stained by Alizarin red. Presented are mouse tibiae, lower jaw, scapulas and spine (Fig. 3.10).

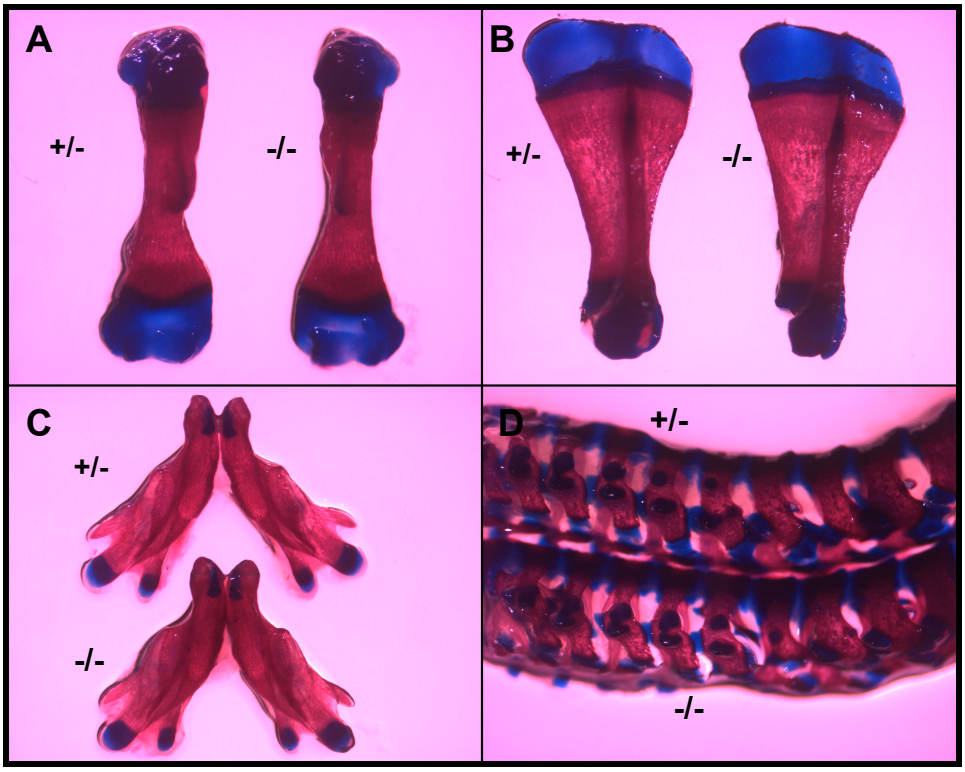

Fig. 3.10 Alizarin red staining of periostin heterozygous (+/-) and homozygous (-/-) mice; Alizarin red staining of the newborn P0 control (+/-) and periostin deficient mice, (A) tibiae, (B), scapulas, (C) lower jaws and (D) spine. Due to the alizarin red-calcium complex formation, calcium-containing tissue is coloured in red and cartilage in blue. Note the similar distribution of cartilage and calcium containing tissues in the mutants and controls.

No significant discrepancies between normal and periostin deficient mice could be detected by this staining method in any of the analysed tissues. Also the shapes and sizes of the cartilages and bony structures were similar. These results suggested that initial bone development in periostin deficient mice was not affected. However, these observations do not exclude the possibility of phenotypes occurring later in life. This requires further investigation.

3.2.4 Molars and incisors of Periostin deficient animals

Periostin expression had been previously demonstrated in the periodontal ligament of adult mice (Hirouchi et al., 1999) and later studies revealed its wide expression in different regions of the teeth and surrounding tissues during embryonic development and postnatal stages (Suzuki et al., 2004; Kruzynska-Frejtag et al., 2004).
The molar tooth germs at cap and bell stage exhibits periostin immunoreactivity in the interface between the more differentiated inner enamel epithelium and the preodontoblasts. Furthermore, at these stages, the dental follicle surrounding the tooth germs also displays periostin immunoreaction. Postnatally, periostin immunostaining is mostly localized in the extracellular matrix and in the dental follicle but not in the cellular elements. In the postnatal incisor, periostin is homogeneously localized in the lingual periodontal ligament and around cementoblasts while the labial connective tissue showed positive periostin staining in the regions adjacent to the papillary layer (Suzuki et al., 2004). This expression pattern of periostin made phenotypes in the teeth or the teeth supporting tissue possible if not probable in periostin deficient mice.

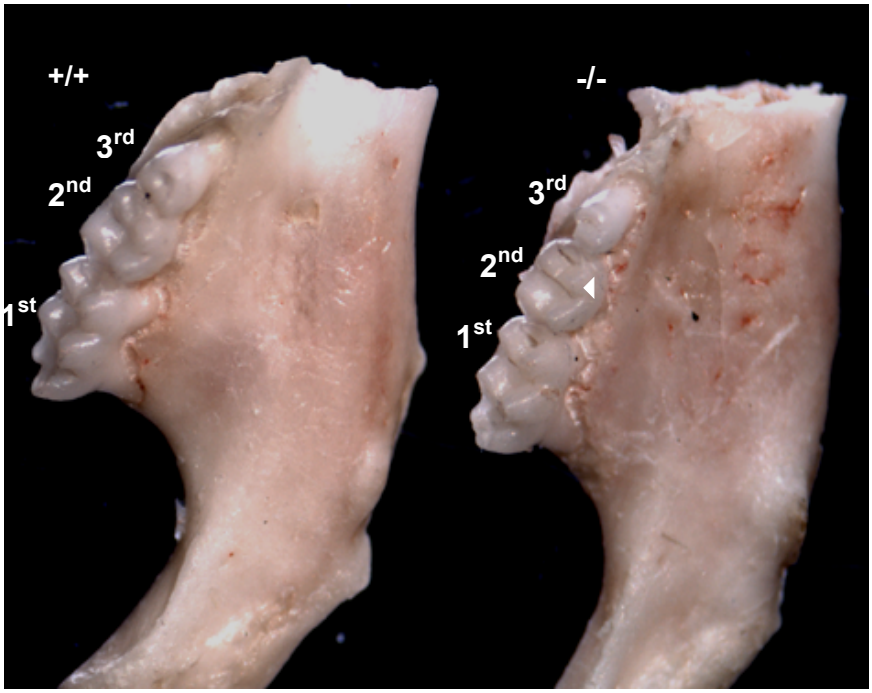

Fig. 3.11 Periostin deficient and normal wild type mandibular molars
Note: the cusps of the periostin deficient molars appear worn out, caries-like structure (arrow heads) and rather smaller overall size of the 3rd molar. Molars alignment are as indicated; x40.

Indeed, Periostin deficient incisors from two months old mice were visibly broken and damaged in comparison to the wt incisors (Fig. 3.13). Periostin deficient molars were affected as well. Their occlusal surface seemed to be worn out in a larger extend than wt mouse molar teeth (Fig. 3.11; 3.12).

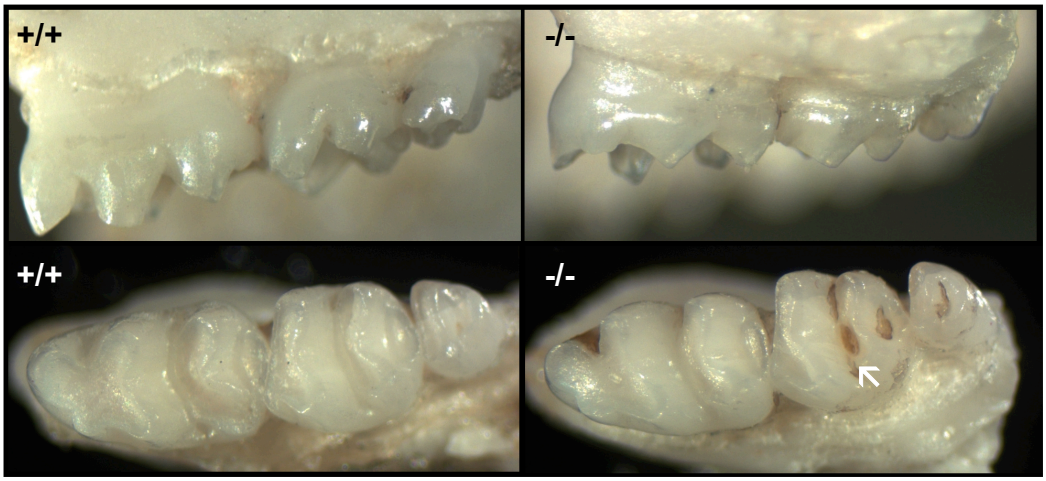

Fig. 3.12 Lateral view of periostin deficient and wild type molars
Note: The caries-like structures (brownish colour) are observable in the periostin deficient molars (see errow).

Fig. 3.13 Periostin deficient and normal wild type mandibular incisors
Note: The broken incisal tip in the periostin null mutant with noticeable appearance of the tooth pulp; x10.

These superficial morphological analyses revealed defects in the teeth of periostin deficient animals affecting the morphology and quality of both, molars and incisors.

3.2.5. Precocious enamel matrix secretion in periostin mutants?

To examine in more detail the observed tooth phenotype in periostin deficient animals, wild type and periostin deficient incisors were cut frontally by a microtome and the sections were stained with haematoxylin/eosin for histological examination. Sections from Periostin deficient and wild type incisors were compared starting from the apical end towards the incisal end covering a length of 3mm. As rodent incisors are constantly erupting, all developmental stages are present on sequential frontal sections beginning with undeveloped stages at apical positions followed by maturing, secretory and finally aged ameloblasts and odontoblasts in more incisal positions. For initial investigations seven and fourteen days old (P7 and P14) wt and mutant incisors were used.

At comparable positions, sections from normal and mutant mandibular incisors at P7 revealed differences in ameloblast and odontoblast developmental stages. At a given distance from the apical end ameloblasts and odontoblasts were not differentiated yet in the wild type incisor as revealed by histological characteristics (cells were not elongated and cell nuclei were not positioned at apical cell end). Additionally no dentin or enamel matrix could be detected (Fig. 3.14A). In contrast on corresponding sections derived from periostin deficient animals ameloblasts and odontoblast showed differentiation characteristics. On these sections the cells were elongated and the production of dentin and enamel matrices had already begun (Fig. 3.14B).

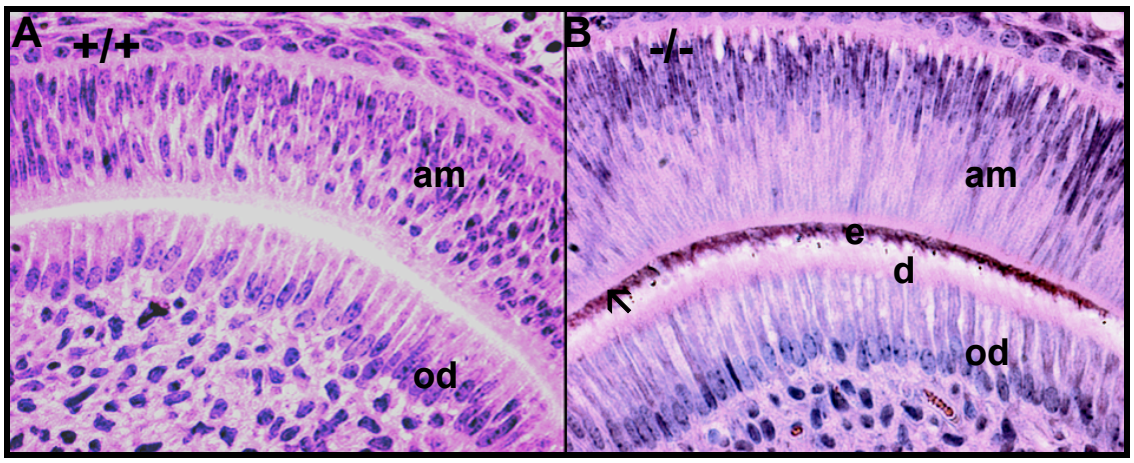

Fig. 3.14 H&E staining of 7 days old control (A) and periostin deficient mandibular incisors (B) Ameloblasts and odontoblasts of the wild type incisor are barely differentiated (only odontoblasts are slightly elongated) and secretion of dentin end enamel matrix cannot be detected (A). Ameloblasts and odontoblasts of the periostin deficient incisor are well differentiated (much more pronounced elongation) and secretion of dentin and enamel matrix has already begun (arrow) (B); am, ameloblasts; od, odontoblasts; e, enamel; d, dentin; x200.

These observations at P7 were corroborated by the results from the sections at P14. Comparing again sections at a given distance from the apical end revealed that ameloblasts and odontoblasts were differentiated and had secreted dentin and enamel matrix in wildtype and mutant incisors. However, the amount of secreted dentin and enamel matrix by periostin deficient ameloblasts and odontoblasts was noticeably higher (Fig. 3.15B) in comparison to the amount of secreted enamel and dentin in the normal incisor (Fig. 3.15A).

These data show that in wild type and periostin mutant incisors at comparable distances from the apical end, odontoblasts and ameloblasts differ in their differentiation state as revealed by histological appearance and matrix secretion. As tooth development involves different processes like migration and differentiation, the exact mechanism by which periostin brings about this phenotype remained speculative and needed further investigations (see 3.3).

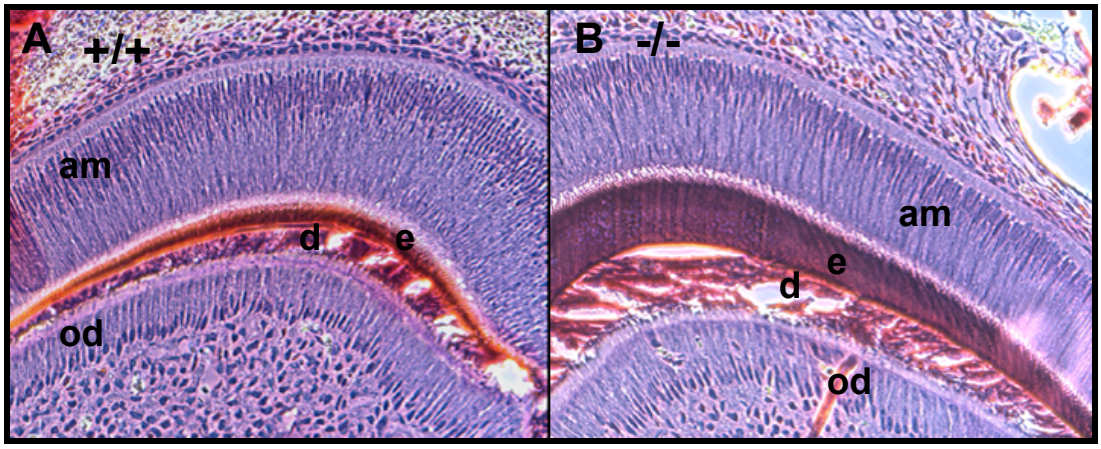

Fig. 3.15 H&E staining of 14 days old control (A) and periostin deficient mandibular incisors (B) The amount of secreted enamel and dentin in periostin deficient mice is significantly higher than the amount of secreted matrix of the normal mice; am, ameloblasts; od, odontoblasts; e, enamel; d, dentin; x 200.

3.3 Severe phenotype of Periostin deficient incisors in the adult

3.3.1 General characteristics

The tooth development in periostin deficient mice during bud, cap and bell stages of embryonic development appeared normal with no significant abnormalities (data not shown). However, they developed a severe tooth phenotype postnatally as already shown (see: Fig. 3.11, 3.12, 3.13). In order to further characterize this defect, I have analysed more postnatal stages focussing on the incisors (Fig. 3.16).

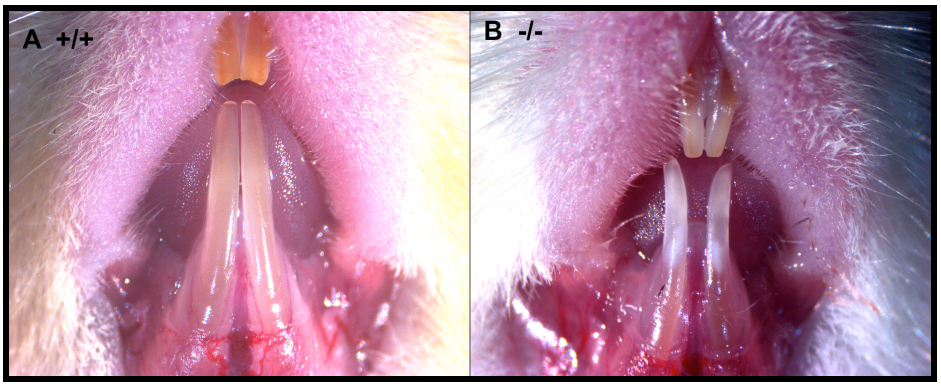

Fig. 3.16 Ventral view of mandibular and maxillar incisors of wt (A) and periostin deficient (B) mice at P60 A chalky white colour of the surface of the mutant incisors indicated hypoplastic or hypocalcified enamel (Fukumoto et al., 2004) or iron deficiency on the enamel surface layer (Yanagawa et al., 2004) Note also the smaller size of especially the mandibular incisors and their abnormal alignment; x7.

The exposed portion of the incisor appeared to be smaller than that of the incisor of the control animals. This difference increased with age, resulting in an anterior open bite, making periostin deficient incisors less efficient for chewing or gnawing.

The colour of normal enamel is influenced by its thickness, translucency and the colour of the underlying dentin. The final brownish, yellowish surface of the incisor is generated by iron deposition from ameloblasts during the last stage of

amelogenesis. The pigment of periostin deficient enamel was lighter and non-homogeneously distributed on the incisor surface. In a previous study, such chalky white colour or translucent enamel surface had been described for hypoplastic or hypocalcified enamel (Fukumoto et al., 2004…)
In the light of these observations, I decided to analyse the appearance of the incisors at different postnatal stages in more detail.

3.3.2 Periostin deficient incisors display malformation and abnormal distortion at the apical end

Microscopic examination of mutant and control littermates showed no significant differences in the dentition up to 10 days after birth**.** This is the age when incisors protrude into the oral cavity. However, incisors isolated from their bony crypt at 2 months of age revealed discrepancies that were increasing with age. These included several abnormalities such as irregular colour and shape of the incisor from apical (root) towards incisal end and abnormal foldings of the tooth at apical (root) end (Fig. 3.17).
Irregular colour of the incisor at the apical towards incisal end suggested that proper development of the different tooth regions, which include enamel and dentin, did not take place.
Enamel secreted by the ameloblasts at more apical positions of the incisor is normally a soft structure. At this stage it contains proteins, which will help in organizing and building up the hydroxyapatite crystals that will later form mature, hard enamel. As it is possible to observe enamel maturation macroscopically, immediately after the tooth is extracted from its bony crypt, I decided to compare wt incisors with periostin deficient incisors. In the wild type, at a position, where enamel had begun to mature i.e. when mineralization had started, it appeared as a white opaque zone (Fig. 3.17). As enamel maturation proceeded further, it changed gradually from white to a yellowish colour. These developmental phase differences, as well as their corresponding lengths, were clearly distinguishable in the wild-type incisors. In contrary, periostin deficient incisors

did not show a clear start of enamel maturation after its secretion phase. The maturation phase overlapped with enamel secretion at the very root end, leading to the observed multiple foldings.

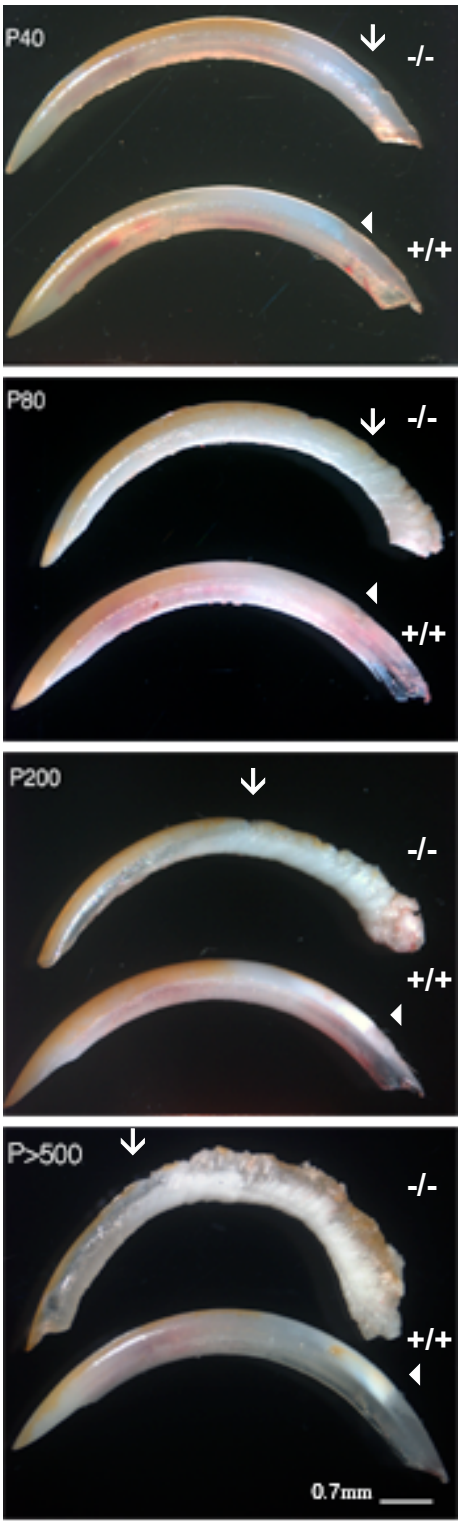

Fig. 3.17 Abnormal foldings of the periostin deficient incisor at the apical (root) end increased with age The start of enamel maturation was clearly observable in the normal incisor as a sharp white opaque zone (arrow heads) (P40 and P80). However, periostin deficient incisors do not display a clear maturation zone at P40 and P80. Instead they show abnormal distortions at the root end. Additionally, this area is a hard, mineralized structure while in wild types this area is soft. With increasing age, the abnormal foldings of the root end extend further towards the incisal end (compare the position of arrows in P40, P80, P200 and P500); x7.

3.3.3 Periostin deficient incisors display premature enamel mineralization

Normal and periostin deficient mandibles were prepared for histological analysis. Sagital and frontal sections, in respect to the incisor length axis, were cut and stained with haematoxylin/eosin. Frontal sections were cut from the beginning of the root end towards the incisal end. Sections at comparable distances from the apical ends were examined.

Histological analysis confirmed that enamel maturation/mineralization spatially overlapped with enamel secretion and thus maturation appeared precocious in comparison to control incisors (Fig. 3.18 A, B, C, D). Starting from the basal end of the normal incisor, it was possible to detect preameloblast and preodontoblasts in frontal section. Ameloblasts were not differentiated and enamel secretion had not occurred yet (Fig. 3.18A). In the corresponding region of the periostin deficient incisor, ameloblasts were found in the differentiated, secretory stage and large amounts of enamel had been secreted. Enamel was not uniformly distributed on top of the dentin layer as in wt incisor (Fig. 3.18C), but it occupied areas of the enamel organ. (Fig. 3.18 I, J).

Approximately 300 μm towards the incisal end of the wild type incisor end, a certain amount of uniformly deposited enamel layer was found on the dentin surface which had been secreted by differentiated, elongated and “regularly distributed” ameloblasts (Fig. 3.18C). Comparable sections derived from periostin deficient animals showed ameloblasts that had stopped to secrete enamel and were already in the maturation phase. Upon entering the maturation phase, ameloblasts lose their secretory capacities and become shorter in length. This phase is also characterized by enamel maturation as well as mineralization.

Further towards the incisal end, fully mineralized, and thus colourless, enamel was found in sections from periostin deficient incisors (Fig. 3.18F) while control incisors still displayed soft, non-mineralized, magenta coloured enamel (Fig. 3.18E).

Additionally, a significantly thicker dentin layer at the expense of the pulp characterized the periostin deficient incisor (Fig. 3.18F, H).

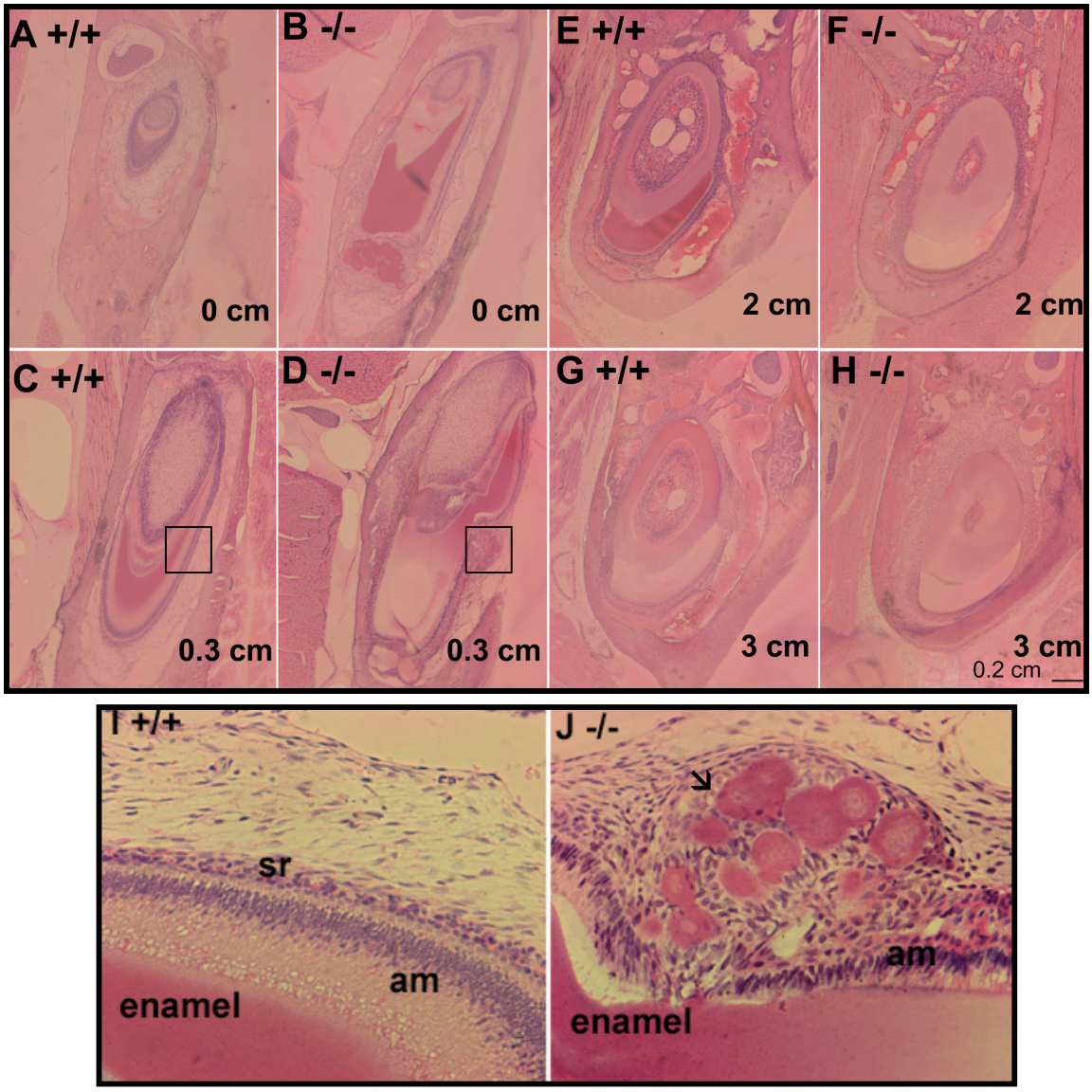

Fig. 3. 18 H&E stained frontal incisor sections from the root end towards the incisal edge at six weeks of age; Shown are regions at the very root end (A, B) where large amounts of enamel matrix was present in periostin deficient incisors. 300μm from the beginning of the root end (C, D) a certain amount of secreted enamel was mineralized. An unusual enamel distribution (enamel globules, see arrow) is shown (I, J) by magnifications of the marked regions in (C, D). The area around 2 cm (E, F) from the apical end revealed soft enamel matrix visible as magenta coloured material in the normal incisor while in the mutant the whole enamel was mineralized and thus colourless. The amount of dentin surrounding the pulp in the mutant was increased thereby making the pulp smaller. This disappearance/closure of the pulp is even more pronounced on sections closer to the incisal end (G, H); am, ameloblasts; sr, stellate reticulum; A-H x40; I, J x200.

In summary, periostin deficient incisors displayed areas where differentiating ameloblasts, still secreting enamel, and ameloblasts, that had already stopped secretion and enamel mineralization had begun, are all present. The normally regularly aligned ameloblast monolayer was found to be severely distorted and misaligned, providing also a plausible explanation for the malformation of the enamel matrix.

3.3.4 Scanning electron microscopy (SEM)

The chalky-white appearance of periostin deficient incisors (Fig. 3.16) suggested possible abnormalities of the enamel and dentin structure. Previously published studies had revealed that chalky-white incisors were hypoplastic or hypocalcified (Fukumoto et al., 2004). Therefore, I decided to examine periostin deficient incisors by scanning electron microscopy. This technique allows the analysis of the enamel layers and the rod distribution on an ultrastructural level. Combined with the energy dispersive X ray analysis (EDX) of enamel and dentin matrices, it also enabled me to determine calcium and phosphate levels in these structures (see chapter 3.3.5).

Mandibular incisors from normal and mutant mice at the age of 8 weeks were embedded in plastic, grinded and without gold plattering analysed by CamScan MaXim 2040S scanning electron microscopy. Again, the incisors were analysed from the apical towards the incisal end.

In the region where enamel was just secreted and not mineralized in the normal incisor, periostin deficient enamel layers were already very strongly calcified, disorganized and malformed. Many such nonhomogeneously calcified, distorted regions were observed (Fig. 3.19).

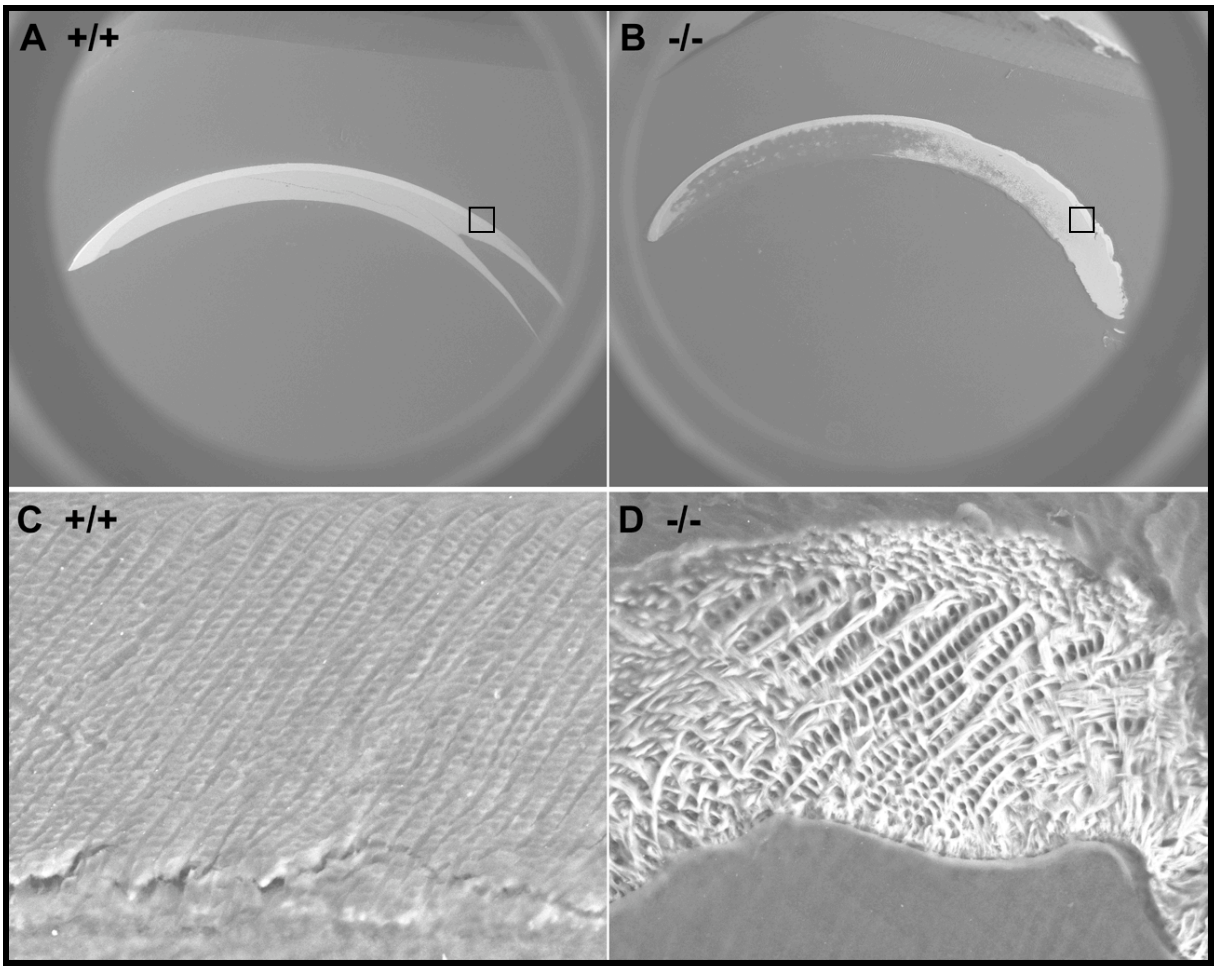

Fig. 3.19 SEM analysis from the apical end of normal (A, C) and mutant (B, D) incisor (P60); The lower panel represents magnifications of the marked areas of the upper panel; x700.

Moving further towards the incisal end, I analysed dentin and enamel layers and found a similar overall structure (data not shown). However, slight differences could be observed. The rods of the periostin deficient incisors always had a more faded, less distinct appearance (data not shown; see also Fig. 3.20). Looking at the incisal end, I could clearly observe that the enamel layer in homozygous mutant incisors was reduced in thickness compared to the control (Fig. 3.20). Additionally, the angle of the rods towards the surface of the incisor varied dramatically between mutant and control (Fig. 3.20).

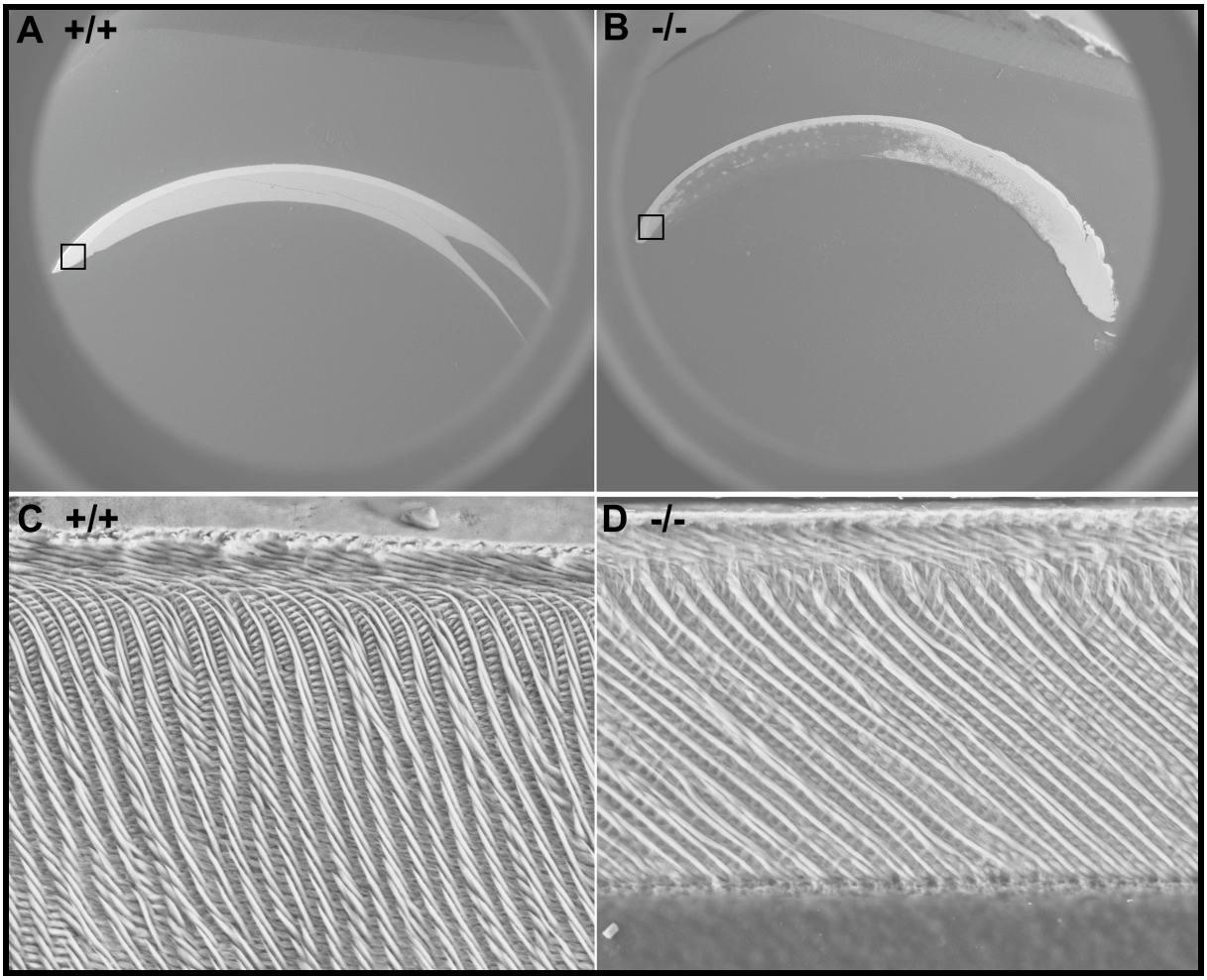

Fig. 3.20 Structural analysis of the incisor cutting incisal edge of the normal (A,C) and periostin deficient (B,D) mice (P60)
Faded appearance of enamel rods in the periostin deficient incisor moving towards incisal end (D) compared to the control (C). Note significantly thinner enamel layer in mutant and an altered angle of the enamel rods; x700.

3.3.5. Energy dispersive X-ray (EDX) analysis

To determine if there is a difference in calcium and phosphor ion levels between normal and periostin deficient enamel and dentin, incisors were analysed spectrofotometrically.

During EDX analysis, the specimen is bombarded with an electron beam inside the scanning electron microscope. The bombarding electrons collide with the atoms′ electrons of the specimen, knocking some electrons off in the process. A higher-energy electron from an outer shell eventually occupies a position vacated by an ejected inner shell electron. In order to change its position, the transferring outer electron must give up some of its energy by emitting X-ray. By measuring the amounts of energy present in the X-rays emitted by a probe, the identity of the atom from which the X-ray was emitted can be established.

EDX analysis of calcium and phosphor ions showed no significant difference in periostin deficient enamel and dentin in comparison with normal enamel and dentin. This was observed at the incisal cutting edge, despite of the incisor age. Furthermore, the same characteristics were observed by analysis of regions towards apical end, where enamel is fully mineralized in both, normal and mutant incisor (Fig. 3.21).

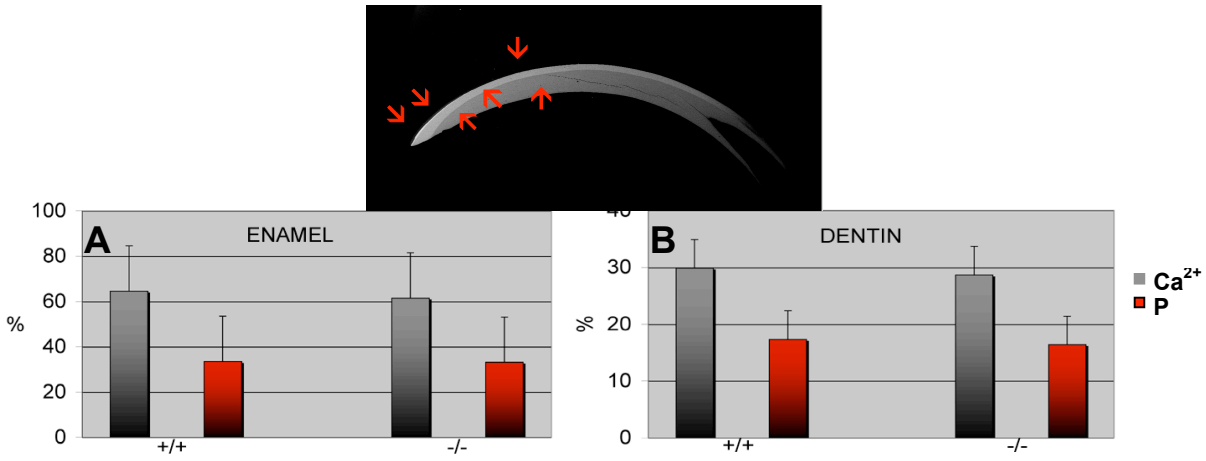

Fig. 3.21 EDX analysis of several different areas of matured enamel in (A) and several different areas within dentin matrix (B) The measurements were performed from the incisal towards the mid region (see errows).

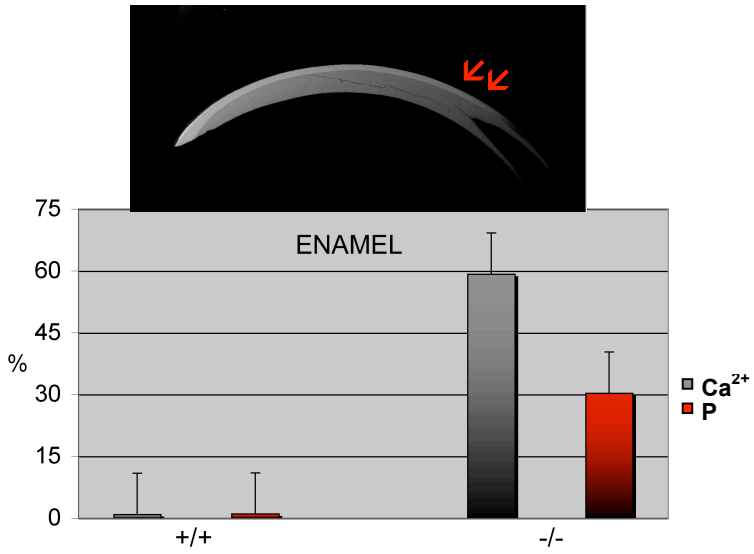

Fig. 3.22 EDX analysis of the matrix at the incisor apical end
The errows indicate apical incisor end where the measuments were performed.

As was expected from our previous results, we found dramatic differences at the apical (root) end. Very high level of calcium and phosphate, comparable to more incisal areas, were detected at the root of periostin deficient incisors while no calcium or phosphate was detectable in normal incisors (Fig. 3.22). This result confirmed our histological and SEM analysis, showing that indeed, the root end of incisors of periostin deficient mice is a highly mineralized structure.

3.3.6 Hardness test

As EDX- and SEM-analysis did not reveal major differences regarding mineralization and overall structure of enamel and dentin layers, respectively, we next examined the hardness.

If the hardness of dentin or enamel is altered it might cause discrepancies in interactions between tooth and PDL. More precisely, Sharpey's fibers of PDL might

not intercalate properly into the cementum. Moreover, the interactions between cementum and dentin might be altered as well. In this study, hardness values were obtained by the Vickers method and conversion tables were used that converted directly the average value of two diagonals into a Vickers hardness value.

Several regions at the root end, fully mineralized enamel region and incisal cutting edge from the normal and mutant mandibular incisors were analysed (Fig. 3.23).

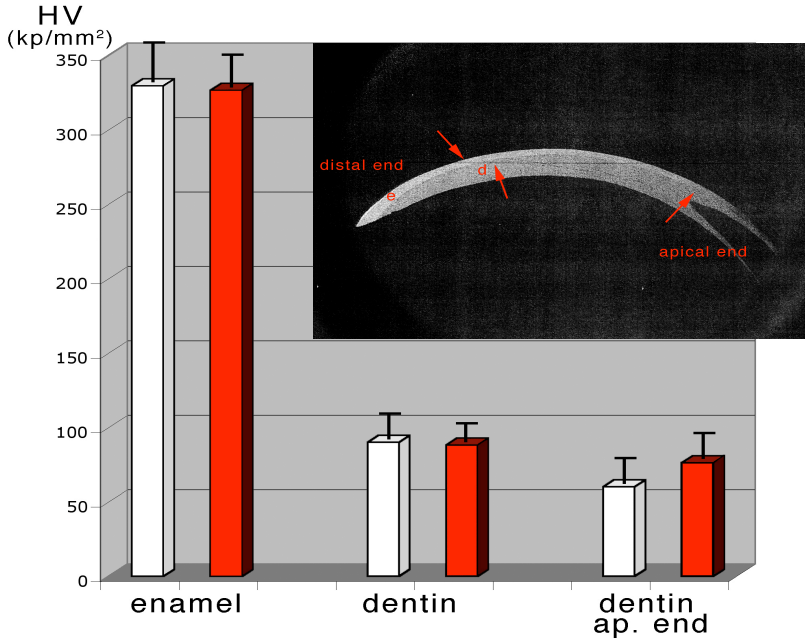

Fig. 3.23 Hardness property of the wild type and periostin deficient enamel and dentin
Presented are the hardness mean values of the control (white) and periostin deficient (red) enamel and dentin obtained by measuring the hardness at the distal end of the incisors. Additionally, the graph shows the ratio between hardness value of the control (white) and periostin deficient (red) dentin at the apical incisor end.

The hardness test did not reveal specific differences in the hardness of periostin deficient dentin and enamel in comparison to the hardness of normal dentin and enamel, thereby supporting the findings regarding the regular characteristics of periostin deficient enamel and dentin by the SEM analysis.

3.3.7 Severe impairment of incisor eruption in periostin deficient mice

Given that mutant enamel structure does not significantly differ from the normal enamel structure, raises the question how such abnormal folding at the apical end of the mutant incisor can develop?

There are several possible explanations. One explanation is that cells of the stem-cell compartement located at the apical end show an enhanced proliferation rate and additionally a premature differentiation. Another possibility is that incisor eruption itself is affected. If the incisor is not pushed or pulled properly in occlusal direction while the stem cells or progenitors are proliferating and differentiating in a normal manner, this would result in a crowding of ameloblasts at the apical end. This in turn could then lead to the observed abnormal foldings of the apical end thereby disturbing the usual incisor development.

As mentioned above, rodent incisors are continuously erupting, which implicates that the attrition at the incisal end is compensated by newly generated material at the apical end. I measured this continuous eruption by marking the mandubular incisors on the labial surface. The movement of this mark in respect to the reference point, the gum margin, was measured (Fig. 3.24). Measurements were performed every five days using six weeks old animals. Mutants were compared with wild type and heterozygous control animals. All animals received powdered food (data not shown), soft food, or hard pellet food (normal), to determine, if different occlusal forces have an effect on the eruption rate. The same experiment was repeated with 18 months old animals that received hard and soft pellet food.

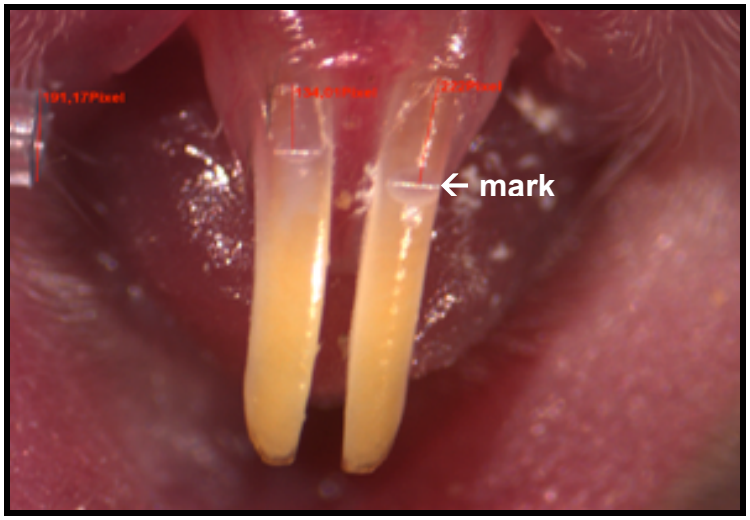

Fig. 3.24 Eruption rate measurements of mouse mandibular incisor
Both incisors were marked on their labial surface. After allowing the incisors to grow for five days, the distance between the gum margin and the mark was measured and recalculated in length value. A plastic tip has been used as a standard; x1,6.

Using this approach, I was able to find a dramatically decreased eruption rate of incisors from periostin deficient mice. In wild type mice, the normal rate of eruption (which equals the rate of wear, so that the incisors remain a constant size in adult mice) is approximately 2 mm/week for the upper incisors and 2.8 mm/week for the lower incisors (Zegarelli, 1944). Autoradiographical studies revealed the rate of euption of MRCTO mouse strain with the mean value of 156 μm/day (Ness, 1965).
My results are in good agreement with these data. Six-week-old animals kept on a hard pellet diet showed an eruption rate of 2,3 mm/week (=0,33 mm/day) of the mandibular (lower) incisors. The eruption rate was slightly reduced to 1,75 mm/week when the animals were kept on soft food (Fig. 3.25). In comparison, homozygous mutant animals kept on hard or soft food displayed a significant decreased eruption rate of 0,21 mm/week and 0,56 mm/week, respectively. Interestingly, the eruption rate in mutant animals decreased when switching from soft to hard food while it

increased in controls (Fig. 3.25). Consequently, the greatest difference in the eruption rate between controls and mutants was present when the animals were kept on hard food (normal nutrition).

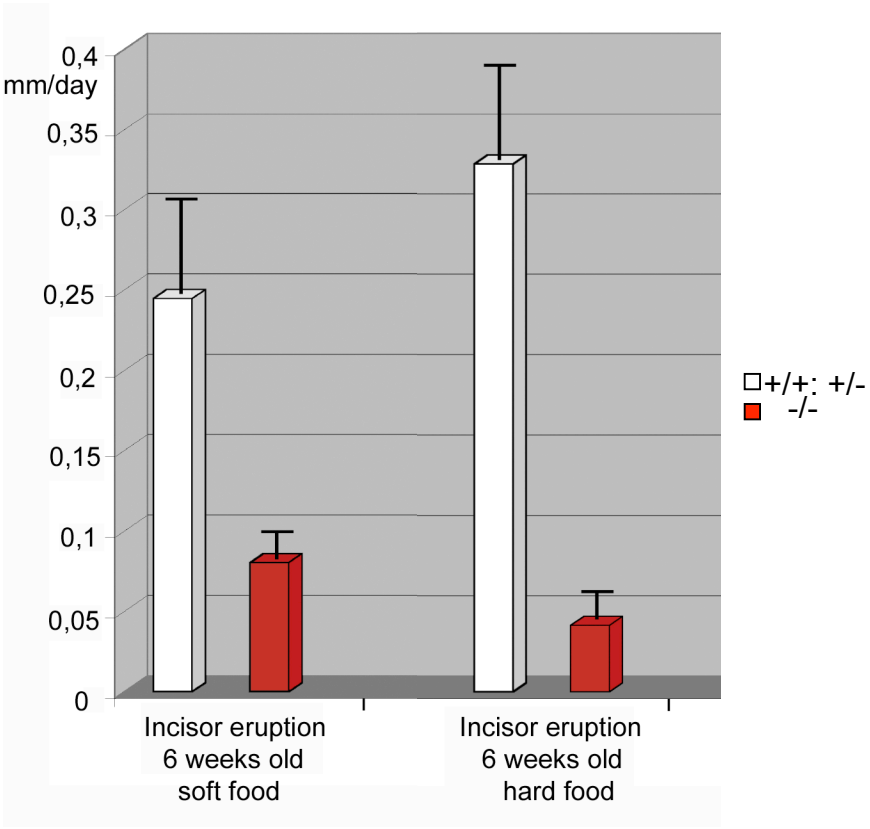

Fig. 3.25 Eruption rate measurements of mandibular incisors in control (+/+, +/-) and periostin deficient animals (-/-); When the animals were kept on soft food, periostin deficient mandibular incisors erupted by a rate that was more than 50 % slower than the rate of eruption of the wild type and heterozygous incisors and more than 90% slower when the animals were given hard food. Measurements were performed every five days. Note: Decreased eruption rate of the control incisors when they were switched from hard to soft food.

Although rodent incisors grow continuously, their rate of eruption declines with age. To examine how the eruption rate of periostin deficient incisor changes with age in respect to the control incisors, I also measured the eruption rate in older animals (age 60 weeks). Interestingly, in periostin deficient animals the incisor eruption rate

was completely arrested while the eruption rate of controls was reduced, as was known from the literature (Berkovitz, 1971; Lavelle, 1969)(Fig. 3.26).

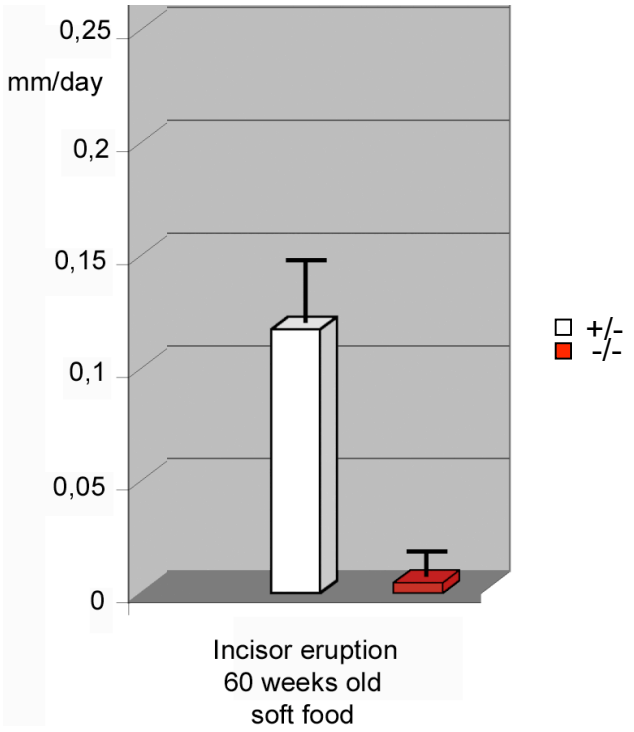

Fig. 3.26 Eruption rate measurements of the 1,5 year old control (+/-) and periostin deficient incisors (-/-); periostin deficient incisor eruption rate is not only decreased, but also arrested at this age. Note: The incisor eruption rate of control mice at this age was reduced in comparison to the incisor eruption rate of the 6 weeks old control mice taking hard food and soft food (Fig. 3.25).

As mentioned before (Chapter 3.3.2), mouse mandibular incisors protrude into the oral cavity approximately between P9 and P10. Given the decrease in eruption rate observed in adult animals, I wanted to determine if the periostin deficient incisors initial penetration into the oral epithelium was delayed. To this end, the incisor eruption rate of 9 and 10 days old mice was carefully examined (Table 3.1).

	Wild type	Heterozygous	Homozygous
+	10	4	0
-	1	10	17

Table 3.1 Note: + protruded; - not protruded into oral cavity

Incisors of all 17 periostin deficient animals examined at P9 were still covered by gum tissue while some heterozygous (4/14) and almost all wild types (10/11) had already erupted (Fig. 3.27). Surprisingly, heterozygous shows an intermediate phenotype, suggesting a clear dosage effect in the early eruption process, which was not apparent during the late eruption process.

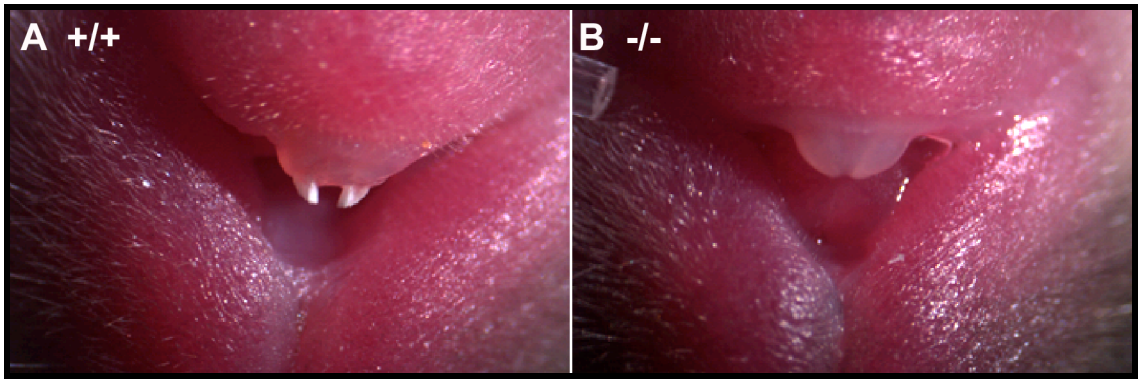

Fig. 3.27 Wild type and periostin deficient incisors at P9/P10
While wild type mandibular incisors were already protruded into the oral cavity (A), periostin deficient mandibular incisors penetration was delayed (B).

My results show that periostin deficiency leads to a reduction of the eruption rate from an early time point on. The eruption rate in homozygous mutant mice is already reduced when the incisors are still completely embedded in the bone, resulting in a delayed penetration. The older the animals get, the stronger this reduction becomes,

leading to a complete cessation of eruption in older animals (demonstrated for 60 weeks old animals).

3.3.8 The periodontal ligament in periostin deficient mice

During embryonic tooth development, periostin is expressed in the dental follicle (Fig. 3.28) and later on in the lingual part of the periodontal ligament (Suzuki et al., 2004)

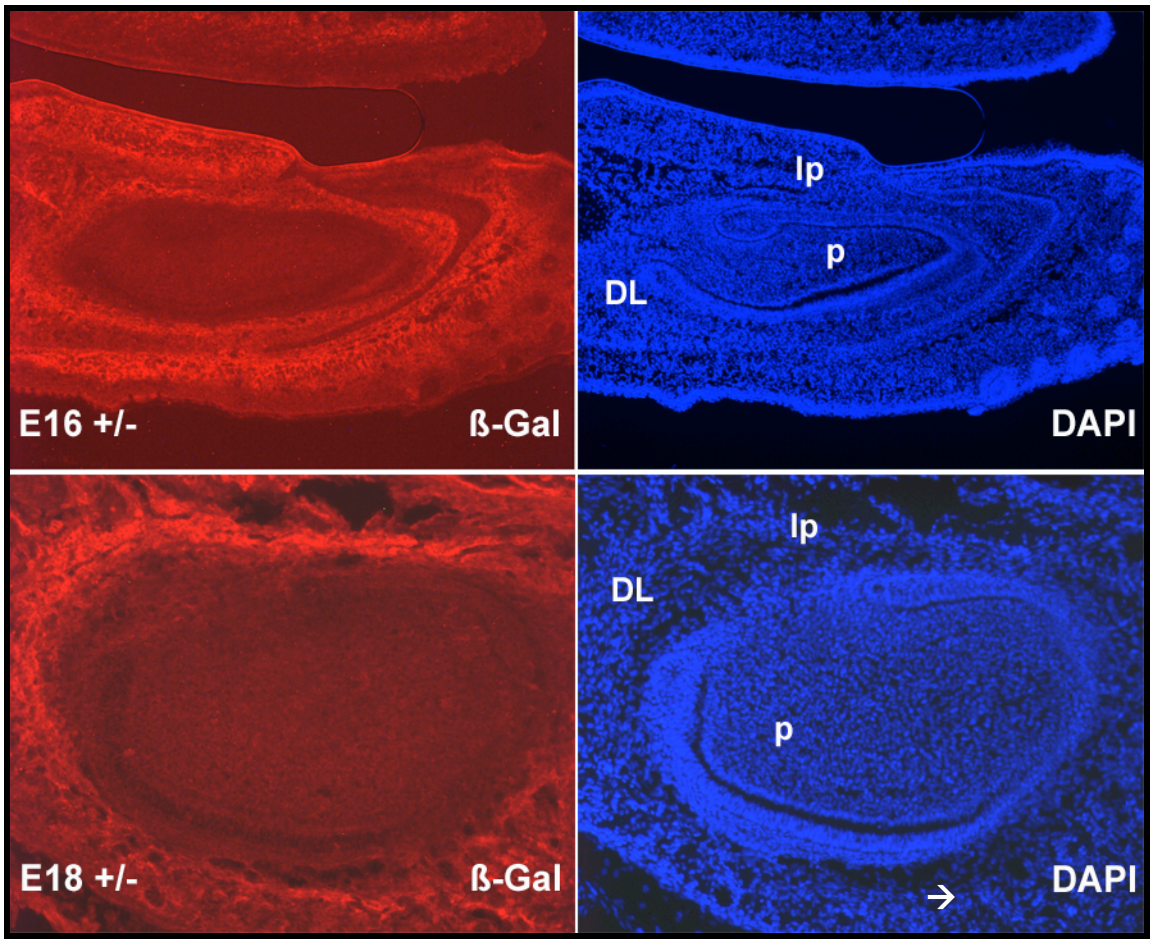

Fig. 3.28 Immunohystochemical localization of periostin in mouse mandibular incisor using ß-galactosidase antibody at E16 and E18. Moderate to strong staining is seen in the tissue surrounding tooth germ, dental follicle; DL, dental follicle; P, pulp; LP, lingual side; right arrow, occlusal direction; x100.

The necessity of the dental follicle for tooth eruption was demonstrated by several studies (Cahill and Marks, 1980; Sandler et al., 1998) In many of these studies it has been shown that abnormal dental follicles can result in unerupted teeth (e.g. Sauk et al., 1998). The dental follicle forms the cementum, periodontal ligament and adjacent alveolar bone.

Periostin deficient periodontal ligament of the six weeks old mice was found to be a highly disorganized structure. A high degree of disorder was observable at the site of interaction between periodontal ligament and adjacent tissues (cementum and alveolar bone). Furthermore, periodontal ligament width was dramatically increased and unusual blood vessels distribution is noticeable (Fig. 3.29).

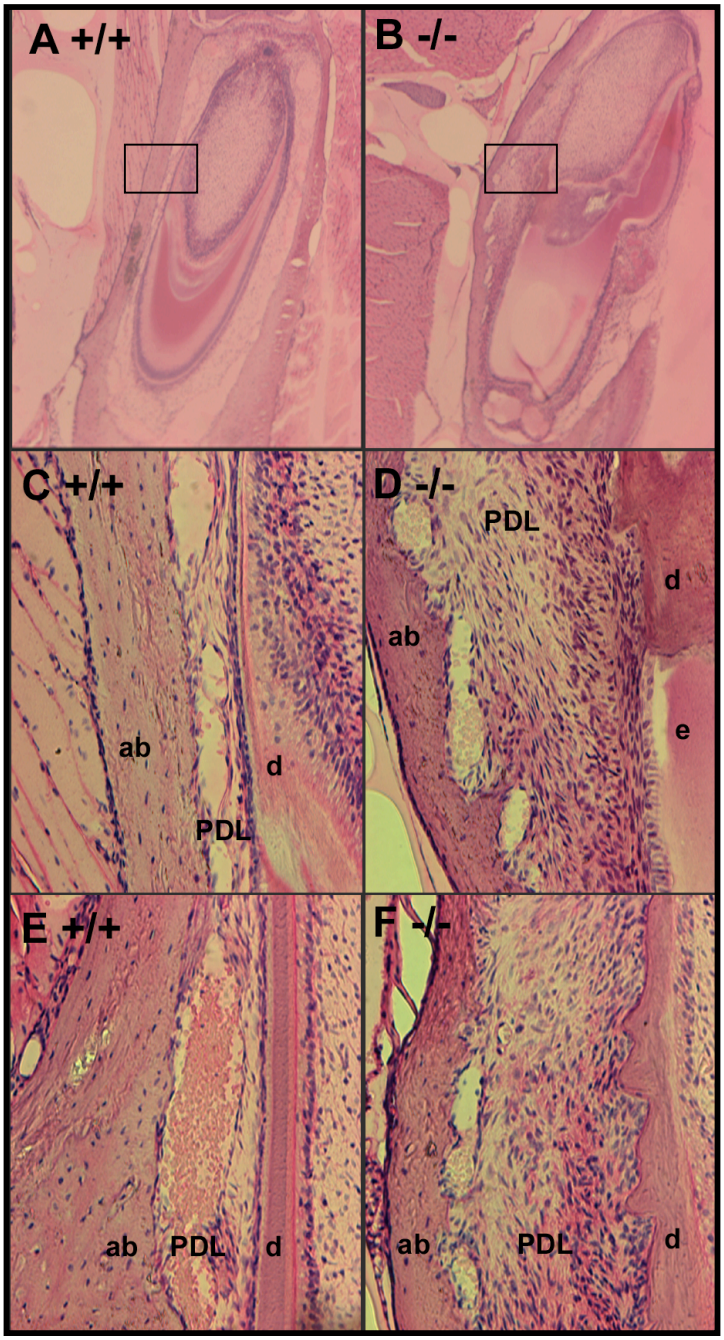

Fig.3.29 Histological analysis of the lingual site of the periodontal ligament from six weeks old wild type (+/+) and periostin deficient (-/-) mice C, D, E, F figures show higher magnifications of the boxed area in A and B. Arrows indicate a disorganized, unclear distribution of the PDL cells as well as a "waved" appearance of the dentin-cementum-PDL-site of interaction. The blood vessels of the mutant PDL were in greater distance from the tooth itself in comparison to the wild-type PDL. Furthermore, the periostin deficient alveolar bone displayed the following discrepancies: The PDL fibers seemed like "protruding" into the bone structure in comparison to the wt alveolar bone characteristics; Note an unusual blood vessels distribution and the alveolar bone structure;
ab, alveolar bone; d, dentin; PDL, periodontal ligament: A, B x40, C, D, E, F x200.

Chapter 4

Discussion

4.1 An overview of the obtained data

In order to elucidate the function of the extracellular matrix protein, periostin, I have generated mice bearing a homozygous mutation of the periostin gene.
I have shown that periostin null mice were born with the expected frequency, however, approximately 25% of the mutants died shortly after their birth.
The restricted expression in periosteum of the bone, periodontal ligament and heart valves during adult mouse life (Horiuchi et al., 1999) helped us to focus our initial examination of the periostin null mice.

One possible cause for the early postnatal morthality might be the expression and requirement of periostin in the heart during embryogenesis or early postnatal life. This analysis is still in progress (see 4.3). Focussing on surviving mutants a crude examination of the skeletal development of newborn mice showed no anomalies in bone and cartilage.
The histological examination of the early postnatal teeth revealed subtle differences. Due to the progressive tooth phenotype in the adult, mainly affecting the incisors, periostin null mice have severe difficulties to chew hard food (normal nutrition) and consequently their body weight decreased and their body size appeared smaller.

As previously published data demonstrated the importance of PDL in continuous rodent incisor eruption (Berkovitz, 1971; Berkovitz and Thomas, 1969) and since periostin is expressed in this tissue during the entire mouse life span, I concentrated on the analysis of the incisor eruption. This study has revealed the importance of periostin in PDL remodelling and maintenance during incisor eruption.

4.2 Generation of periostin deficient mouse line

The targeting vector was prepared by in-frame insertion of the LacZ gene into the open reading frame (orf) of the periostin gene, thereby deleting sequences of the periostin gene resulting in an inactivation of periostin gene expression. Homologous recombination of the targeting vector in murine embryonic stem cells was achieved using standard protocols. The mutant allele was transmitted into the germ line and thus a mouse line that carries this mutation could be established. Periostin mutants, heterozygous and null mutants, were identified by Southern Blot analysis and later routinely by PCR. To verify the null mutation on the protein level, a Western Blot analysis was performed using adult dentin tissue, as periostin is highly expressed in this tissue. Using extracts of this issue the absence of Periostin in homozygous animals could be demonstrated. LacZ gene expression as revealed by ß-galactosidase activity in the Periostin mouse strain followed exactly the periostin expression pattern that had previously been analysed by in-situ hybridization with periostin specific probes and immunohistochemistry using periostin specific antibodies (Michaela Miehe, Dissertation, Hamburg 2003 and unpublished data). Therefore, apart from helping to understand the biological functions of periostin, this mouse line presents a useful tool to study the expression pattern of periostin in great detail. On the one hand the origin of periostin expression can be determined, by the presence of ß-galactosidase, which remains inside the cell that synthesizes it, while the location of the secreted periostin on the other hand can be identified by specific antibodies.

4.3 Early postnatal lethality of the periostin deficient mice

Initial observation of born animals revealed that the rate of surviving mutant animals was decreased by approximatelly 25%. During all stages of embryonic development, however, I found the expected Mendelian ratios. This pointed towards an early postnatal lethality of some homozygous mutants. One of periostins expression domains that could be implicated in the observed mortality is the heart (Kern et al., 2005; Kruzynska-Frejtag et al., 2001; Litvin et al., 2005; Norris et al., 2004). The heart becomes vitally important during midgestation. Several mouse mutants with defects in tissues of the heart have demonstrated that these mutations can cause embryonic or postnatal lethality depending on the severity of the evoked defects (Wessels and Sedmera, 2003). We have detected histological abnormalities in some homozygous mutant hearts that could potentially account for the observed lethality. However, as the penetrance of lethality is only 25%, the phenotype is difficult to analyse. If the observed abnormalities can be correlated to the mortality and the exact mechanism underlying this lethality, remains to be clarified in further experiments.

4.4 Initial analysis of the periostin deficient mice

Surviving mutants were smaller and had a significantly reduced body weight. As periostin is expressed in the periosteum, I decided to analyse the skeletal development. In this study, I used Alizarin red staining and found that periostin deficient newborn mouse skeletons revealed no significant abnormalities in the bone and cartilage. My data were confirmed by another group that had also created a periostin-knock-out model (Rios et al., 2005). In this study the authors similarly found that Alizarin red staining of newborn skeletons showed identical skeleton size and

structure of mutant and wildtype littermates. No differences in length and diameter of newborn forelimbs and craniofacial region were found. In search for other possible explanations for this phenotype, I investigated the metabolism of the mutants in specially designed metabolic cages. This experiment showed that the metabolism was unaltered in homozygous mutant animals and therefore cannot account for the size and weight reduction.

The tooth phenotype observed in homozygous mutant animals that is discussed in detail below finally provided an explanation for the reduction in size and weight. Indeed, when mutant animals, that had severe difficulties to chew the normal hard pellet nutrition, were kept on soft food they displayed almost normal size and weight. This indicated that the observed reduction in size and weight was a secondary effect of the tooth defects and not a primary consequence of the periostin deficiency. This almost complete rescue was also confirmed in the other study (Rios et al., 2005). So, despite the high expression of periostin in the periosteum there are no major changes in cartilage and bone formation or maintenance. Subtle phenotypes cannot be completely excluded and thus require further more detailed investigations.

4.5 Tooth phenotype in periostin deficient mice

Initial observation of the periostin deficient mouse molars and incisors revealed their abnormal appearance. The occlusal surface of the mouse molars appeared worn out and the size of the 3rd molar was decreased. Periostin deficient incisors were noticeably broken with visibly exposed pulp chambers. Histological analysis of six weeks old periostin deficient incisors displayed an increased amount of secreted enamel and dentin in comparison to the normal incisors at comparable positions. Two models can explain the incisor phenotype of periostin deficient mice. The first model is based upon premature differentiation of ameloblasts and odontoblasts, whereby

enamel and dentin are secreted sooner, which might lead to their accumulation. The second model is based upon a spatial shift of the developmental stages due to an alteration in the eruption rate.
The seemingly premature secretion of enamel, lead me to analyze this structure more thoroughly. SEM analysis revealed a regular enamel layer distribution of the periostin deficient incisors as in the control incisors with some discrepancies moving towards the incisal end. These include a considerably thinner enamel of the periostin deficient incisors that have a faded appearance, which was accentuated with age. Additionally, an altered angle of the enamel rods is observable, which might contribute to the overall thinner enamel in mutants. A thinner enamel of the periostin deficient incisors is inconsistent with the first model of premature cell differentiation in mutant incisors, since that should result in thicker enamel.
This inconsistency indicates that another aberrant developmental process could be responsible for the observed phenotype and therefore favoring the second model.

These discrepancies observed with SEM analysis could be the cause of periostin deficient incisor's "higher sensitivity", i.e. chewing and exposure to the bacteria (acids). Periostin deficient incisors do not have a sharp incisal edge as wild type incisors do (Wang et al., 2004). The incisal edge differs in shape and form and this dissimilarity increases with age, suggesting that enamel is wearing out faster than in wild type. As I have focused on the incisor, it cannot be excluded that changes in the enamel structure of the molars could be causative or contribute to molar defects as well, which remains to be determined.

In contrast to the SEM analysis, no differences were detected by EDX analysis and Vickers hardness test, which showed that in the enamel and dentin the calcium and phosphor levels and hardness of the mutant incisors are not significantly altered and are comparable between the mutant and the wild type incisors with the exception of the apical root. In this region, I could observe, in good coordinance with the histological data, a major difference between homozygous mutant and wildtype

incisors. The histologically observed “premature” secretion and mineralization, in this region, is mirrored by the EDX analysis, which revealed that, indeed, the apical ends of the mutant incisors contain high amounts of calcium and phosphor ions, demonstrating a mineralized structure. The unaltered overall hardness of the incisors in the periostin deficient animals cannot explain the observed defects of the incisors again pointing towards changes in the eruption rate being causative.

Histology, SEM, EDX analysis and Vickers hardness test are interesting and coherent results, but they do not explain the cause of the periostin deficient incisor phenotype (see chapter 4.6).

4.6 Eruption disturbance of the periostin deficient incisors

Tooth eruption is the developmental process when the tooth moves from its place of development in the alveolar crypt to its final functional position into the oral cavity. In rodents, the molars are characterized by limited eruption. In contrast to molars, the rodent incisors erupt continuously and thus require different developmental events in comparison to the molars.

As already mentioned in chapter 4.5, a possible explanation for the observed phenotype could be an alteration in rate of tooth eruption. In support of this, some previously published data on the mouse incisors showed very similar findings with mine. The analysis was performed on the rat incisor after hypophysectomy (Schour, 1934). The incisors were distorted in form, had multiple foldings at their apical end and the pulp was almost closed by the increasing dentin structure towards the incisal edge. One of the additional incisors characteristics after the hypophysis removal was a retarded eruption rate very soon after the operation. Thus, a very similar phenotype

to mine correlates with delayed incisor eruption. Therefore, I analysed the eruption rate of incisors in periostin deficient mice.

The measurements in adult mice showed that in periostin deficient incisors, the continuous eruption process is affected. The initial penetration into the oral cavity is slightly delayed indicating that already at early phases of the eruption movements; the eruption process/mechanism is altered. The ongoing continuous eruption rate becomes gradually slower until it finally stops.

These findings provide a clear explanation for the observed Periostin deficient incisor phenotype and are consistent with the observed histological data.

As a result of this deceleration of the eruption process, ameloblasts and odontoblasts generated at the apical end cannot move along the eruption axis. Thus, ameloblasts accumulate at the apical end. As their differentiation is not significantly altered they soon start to produce enamel thereby causing the abnormal mineralization and the ruffling at the apical ends. In time, the accumulating ameloblasts are forced by space constraints along the incisor axis explaining the progression of the abnormal ruffles and foldings towards the incisal end with age. The odontoblasts similarly accumulate inside the pulp chamber and thereby cause with increasing age the progressive closure and complete mineralization of the pulp towards the apical end. Most likely, the widening of the PDL (Fig. 3.29 and see below) can also be explained by accumulating PDL cells.

Finally, the histological observation (Fig. 3.14, 3.15) that suggested precocious differentiation of ameloblasts and odontoblasts can also be explained by this deceleration of the eruption process as it results in the appearance of fully differentiated ameloblasts at unusual, more incisal positions with time.

The whole mechanism of tooth eruption is still poorly understood. Most experiments regarding tooth eruption were performed on the rodent incisors, whose eruption mechanism might not be identical to the eruption process of teeth with limited growth (rodent molars). It is evident from many previous studies that tooth eruption is a complex process, which requires many factors. Proposed factors include cell

proliferation, blood pressure, bone resorption and the PDL. In rodents, it was shown that removal of the apical incisor end, thereby excluding the apical stem cell compartment, did not affect the remaining part of the incisor to erupt, suggesting that stem cell differentiation or proliferation are not essential for the eruption process. Blood pressure might be involved, although it was shown not to be essential (Main, 1966). Through the years, much attention has been given to the PDL as the main contributor for the incisor eruption (Berkovitz, 1971; Berkovitz and Thomas, 1969; Melcher, 1967; Ness, 1965). Autoradiographical studies demonstrated active movements of the PDL fibroblasts while the incisor erupts (Beertsen, 1975). It has been reported that in the lingual part of the PDL of rodent incisors, migration of fibroblasts and fibers occurs in occlusal direction with a rate equal to the incisor eruption rate, suggesting that PDL fibroblasts might pull out the tooth during eruption (Beertsen, 1975). Moreover, it has been suggested that collagen remodelling plays a crucial role in maintaining the integrity of the PDL during eruption (Everts, 1988). However, experiments in which the collagen network was inhibited and the connection to the tooth was disrupted, demonstrated that the PDL is not the crucial factor for the tooth eruption (Berkovitz, 1972). Finally, the hormons seems to be important for tooth eruption as shown in experiments performed after hypophysectomy in rats (Schour, 1934).

During tooth eruption, the remodelling of the periodontal and gingival connective tissues take place (Ten Cate et al., 1976). It was suggested that remodelling in the PDL is particularly restricted to the shear zone, an intermediate region of the PDL, where fibers from the bone and fibers from the tooth intermingle, (Sicher, 1942). Remodelling requires a coordinated breakdown and synthesis of extracellular matrix (ECM). Moreover, PDL fibroblasts respond to the application of mechanical forces (eruption and orthodontic movements) by significantly increasing production of collagen type-I and fibronectin (Howard et al., 1998).
Recently, it was reported that undigested collagen fibers in the shear zone of the PDL

were accumulated in periostin deficient mice, suggesting that the collagen fibers digestion in the PDL shear zone is significantly important for the incisors to erupt (Kii et al., 2006). The authors report a direct protein-protein interaction between collagen typeI and periostin. Thus, it can be speculated that periostin affects the collagen turnover thereby facilitating the formation of new ECM-ECM or ECM-cell interactions, which in turn are necessary to accommodate for new positional changes of the tooth caused by the eruption movements.

The histological data obtained in this study demonstrate a widening of the PDL with age and abnormal foldings of enamel and dentin that probably affect the interaction of PDL cells and fibers (e.g. Sharpey's fibers) with the incisors (See chapter 3.3.8, Fig. 3.29). Previously, it was suggested that PDL fibroblasts might play a role in pulling the tooth axially by means of the network of collagen fibers (Beertsen et al., 1974) and Kii et al have recently demonstrated changes in the collagen network especially in the shear zone of periostin deficient animals (Kii et al., 2006). Although these findings are very suggestive, experiments were the collagen turnover was experimentally inhibited or interaction between the PDL and the incisors were abrogated showed no alterations of the eruption velocity (Berkovitz, 1972). Thus, it is more likely that the collagen network is required for stabilizing the incisor in its current position rather than being important for mediating the movement. If this is the case then the finding of changes in the collagen network in periostin mutant animals (accumulation in the shear zone) suggests that absence of Periostin leads to "over-stabilization" of the incisors thereby slowing down the eruption and finally with increasing age making eruption impossible.

In my Ph.D.thesis, I concentrated on the analysis of the incisor phenotype. However, the homozygous mutant molars also show differences when compared to wildtype. In rodents, the eruption of the molars is different to the eruption of the incisors. It will be interesting to analyse the eruption of the molars in the periostin deficient mice, particularly since an increased expression of periostin message was detected in the

pressure sites of the upper first molar following mechanical stress (Wilde et al., 2003). This indicates a possible upregulation of periostin by uptake of higher mechanical force or during eruption. The eruption rate data of the periostin deficient molars combined with the already obtained eruption rate data of periostin deficient incisors could provide new insights on the developmental eruption mechanisms occurring in both. We could learn weather the eruption process between molars and incisors share one general eruption mechanism or if there might be a different mechanism during incisors eruption that would enable the continuous eruption process. It can be speculated that in the latter case, the different developmental eruption mechanism, which enables continuous eruption in the incisor, is periostin dependent and thereby causes the delay and deceleration of incisor eruption in periostin deficient animals.

The complete mechanism by which Periostin performs its function is still not fully solved and remains to be further investigated. Periostin contains a cysteine rich EMI domain, which is shown to participate in multimerization (Doliana et al., 2000). It might interact with other proteins (integrins, collagens) as a multimer, thereby providing a scaffold by which signals for PDL remodelling (cell proliferation, differentiation, enzyme secretion, ECM degradation and secretion) might be influenced. The periostin deficient mouse line generated in this study provides a useful tool for further investigating the eruption process. Whatever will be discovered in future experiments, it is undoubtful that periostin is an important player in PDL remodelling during tooth eruption in mice.

Chapter 5

Material and Methods

5.1 Materials

5.1.1 Enzymes

The following enzymes were obtained by Stratagene, MBI Fermentas, Sigma, Roche, Clontech and Invitrogen:

PfuTurbo DNA polymerase; Stratagene
Taq DNA polymerases; (polymerase mixtures); Invitrogen
T4 DNA Ligase; Roche
Schrimp alkaline phosphatase (AP); Roche
Restriction enzymes; MBI Fermentas, NewEngland BioLabs
Rnase; Sigma

5.1.2 Cloning Vectors

PTVFlox-O; D.Riethmacher
PBluescript-SK II (+/-); Stratagene
PGEM-Teasy; Promega

5.1.3 Eukaryotic Cell line and Bacteria strains

Embryonic stem cells from the129/Ola mouse strain E14.1 (Kuhn R., 1991)
*E.Coli,*XL1-BlueMRF(Jerpseth,1992)

5.1.4 Chemicals and Bioreagents

Standard chemicals were supplied by Merck, Roth or Sigma.

Anaesthetic solution

2,2,2 Tribrom-ethanol	1 g
2-methyl-2-butanol	620 µl
H_2O	79 ml

Denhardts solution (50x)

Ficoll 400	50 g
Polyvinilpyrrolidon	50 g
BSA	50 g
H_2O	1l

Southern Blot-prehybridization solution

20x SSC	30 ml
50x Denhardts	10 ml
Salmon sperm (9.6 mg/ml)	25 µl
10% SDS	5 ml
H_2O	54,975 ml

Southern Blot-denaturation buffer

NaCl	1,5 M
NaOH	0,5 M

Southern Blot-neutralisation buffer

NaCl	1,5M
TrisCl	0,5M

Western Blot –blocking buffer

Instant milk powder 5% (w/v) in PBS

Western blot-blotting buffer

Tris	25 mM
Glycine	190 mM
Methanol	10 % (vIv)

Sample buffer-protein gels

Tris-Hcl pH 6.8	0.312 M
SDS	10 % (w/v)
ß-Mercaptoethanol	5 % (w/v)
Glycerol	50 % (v/v)
Bromphenol blue	0.13 % (w/v)

SDS running buffer-protein gels (10x)

Tris HCl pH 8.3	0.25 M
Glycine	1.9 M
SDS	1 M

SSC (20x)

NaCl	3 M
Natriumcitrat pH 7.0	0,3 M

TAE (50x)

Tris-Acetat pH 8.0	2 M
EDTA	100 mM

LB-Medium

NaCl	10 g
Bacto-Trypton, pH 7.3	10 g
Yeast extract	5 g
Add H_2O to 1000 ml, adjust pH 7,5 with 10 M NaOH and autoclave	

LB/Amp-medium

Ampicilin in LB-Medium	100 μg/ml

LB/Agarplates

Agar in LB-Medium	20 mg/ml
Ampicilin	100 μg/ml

5.1.5 Cell culture

PBS (10x, 1000ml)

NaCl	100 g
Kcl	2,5 g
$Na_2PO_4xH_2O$	7,2 g
KH_2PO_4	2,5 g
Add to 900 ml H_2O, set pH 7,2 with 10 M NaOH; Add H_2O to 1000 ml. Dissolved 1:10 and autoclaved	

FCS/FBS; (HyClone/Gibco)

Heat-inactivated at 55°C for 30 min

Fibroblast cell medium (FC)

Dulbecco MEM with Glutamax-I, 4,5 g/L Glucose, Pyridoxyn, Natriumpyruvat; Gibco	434 ml
FBS; Gibco	50 ml

Non-essential Aminoacids (100x); Gibco	5 ml
Penicilin/Streptomycin (100x); Gibco	5 ml
L-Glutamine 200 mM (100x); Gibco	5 ml
β-Mercaptoethanol 50 mM; Gibco	1 ml

MitomycinC (2 mg packing bottle)

Dissolve in 0,1 ml DMSO and 1,9 ml PBS;
40 µl/ 10 ml FC-Medium (f.c. 4 µg/ml)

ES cell medium (EC)

Dulbecco MEM with Glutamax-I, 4,5 g/L Glucose, Pyridoxyn, Natriumpyruvat; Gibco	408,5 ml
FCS; HyClone	75 ml
Non-essential Aminoacids (100x); Gibco	5 ml
Penicilin/Streptomycin (100x); Gibco	5 ml
L-Glutamine 200 mM (100x); Gibco	5ml
β-Mercaptoethanol 50 mM; Gibco	1 ml
LIF (Leukemia Inhibitory Factor)	0,5 ml

LIF was generated by a stably transfected CHO-cell line
that expresses the human cDNA.
Supernatants were collected and used in 1:5000 dillution.

Fibroblast/ ES cell freezing medium (10 ml, 2x)

DMSO	2 ml
FCS	1 ml
EC medium	7 ml

Gelatine (0,5%)

Gelatine	2,5 mg

Dissolved in 500 ml H_2O and autoclaved

5.1.6 Histology and immunohistochemistry

Fixation solution for Immunohistochemistry

Paraformaldehyd	40 g
PBS	1 l

X-Gal-detergent buffer (1000 ml)

$MgCl_2$	200 µl (2 mM)
Na-desoxycholat	100 µl (0,01%)
Igepal or Nonidet	200 µl (0,02%)
Phosphat buffer pH 7,3; 0,1 M to 1000 ml (Stocks solutions; 1M Na_2HPO_4, 1M NaH_2PO_4)	

X-Gal-staining solution (10 ml)

X-Gal (20 mg/ml in DMF)	500 µl (1 mg/ml)
K-Ferricyanid (500 mM in PBS)	100 µl (5 mM)
K-Ferrocyanid (500 mM in PBS)	100 µl (5 mM)
X-Gal-detergent buffer to 10 ml	

Methylmetacrylate-preinfiltration solution

Technovit 7100 (Heraeus-Kulzer) in 100% EtOH	1:1

Methylmetacrylate-infiltration solution (100 ml)

Hardner 1 (Heraeus-Kulzer)	1 g
Technovit 7100 (Heraeus-Kulzer)	100 ml

Methylmetacrylate-embedding solution

Methylmetacrylate-infiltration solution: Hardner II (Heraeus-Kulzer)	15:1

Haematoxylin staining solution

Mayer's hemallaun (Sigma)

Eosin staining solution (100 ml)

Eosin	400 mg (0,4%)
H_2O	100 ml

Antibody solution (100 ml)

PBT	0,1%
Goat serum (Sigma)	1 ml (1%)

PBS/Tween 20 (PBT)

PBS (10x)	100 ml
Tween 20	1 ml (0,1%)
Add H_2O to 1000 ml	

Blocking solution (100 ml)

PBT	0,1%
Goat serum (Sigma)	10 ml (10%)

Primary and secondary antibody

Rabbit polyclonal ß-Galactosidase antibody; Abcam (ab616)

Rabbit anti-periostin serum (Michaela Miehe)

Goat anti-rabbit IgG, Cy3 conjugated; Dianova (111-165-045)

Goat anti-rabbit IgG, Peroxidase conjugated; Dianova (111-035-045)

5.1.7 Oligonucleotides

Primers for cloning „long arm“ homology of the targeting vector

Osf 3900f	5′ -ACA GAG AAT ACC CGC AGA GG- 3′
Osf 3900fNotI	5′ -ACA GAG A**GC GGC CGC** AGA GG- 3′
Osf 3576r	5′ -GAG GCC AGG TCA GAA GAG TG- 3′
Osf 3330f	5′ -CAT CTT CCC GAC TGG TAG GA- 3′
Osf exon1r-	5′ -GGA ACC ATC TTC AGC CCT GAGC- 3′
Osfexon1r NruI	5′ -**TCG CGA** GCC ATC TTC AGC CC- 3′

Primers for cloning „short arm“ homology of the targeting vector

Osf 7404f	5′ -GTT CTG CAA GCT CGC CCC TTC CCC AG- 3′
Osf 7404SalI	5′ -CCC CAG **GTC GAC** TTT TTC TGC- 3′
Osf long arm 5r	5′ -TCA TGC ATG CAC ACA CTG TT- 3′
Osf8650AscIr	5′ -CCT GCG **GGC GCG** CCT TTC ATC CC- 3′

Primers for genotyping periostin-deficient mouse line

Primers for the 531 bp wild type allele:

5′ -TGTGGTGGCAGAGACAGAAG- 3′

5′ -CTCCCCTGTGGTGCATTTAC- 3′

Primers for the 775 bp mutant allele:

5′ -TGTGGTGGCAGAGACAGAAG- 3′

5′ -GTTGCACCACAGATGAAACG- 3′

5.2 Methods

Molecular biology standard methods were performed according Sambrook et al., (1989) unless it is stated differently.

5.2.1 Molecular Cloning

DNA digestion with restriction endoclucleases

DNA was digested according to manufacturer instruction in 20-100 μl total volume.

DNA dephosphorilation

5′-Phosphate groups from linearized vector were removed at 37°C for 2h with alkaline phosphatase (CIP). After cleaning and isolation from the agarose gel, final DNA concentration was estimated on an agarose gel by comparing with MW standards.

Ligation of DNA fragments with T4-Ligase

Ligation of plasmid vectors and DNA fragments was performed at 16°C water bath overnight using a plasmid vector : DNA fragment ratio 1:3 (Crouse et al., 1983).

Phenol/Chloroform-Extraction

In order to eliminate the proteins and inactivate enzymes in DNA mixtures, the sample was mixed 1:1 with Phenol/Chloroform. After centrifugation at >13000xg for 10 min, the upper DNA containing phase was isolated. Finally, the DNA was precipitated in ethanol.

Production and transformation of competent XL1-Blue bacteria

Competent cells were prepared according to Inoue et al. (1990). 200 μl of competent cells were defrozen on ice. Incubation with10 μl of ligation mixture was performed on ice for 30 min. After 30 min, the cells were heat shocked at 42 °C for 1 min and placed on Ampicilin LB-Agar plates that were prepared for blue-white selection with X-Gal/IPTG.

Preparation of Plasmid-DNA

Plasmid Mini-preparations were based on alkaline lysis according to Birnboim et al. (1979). For the large scale, plasmids were isolated with Plasmid-Maxi-Preparations –Kit (Qiagen, Hilden).

Agarose gel electrophoresis

0,7-2% agarose gels were prepared to separate 0,5 and 15 kb DNA fragments. Agarose was dissolved in 1x TAE Buffer, mixed with ethidiumbromide (final concentration; (f.c.) 1 μg/ml) and poured into a gel chamber. Before loading, the DNA solution was mixed with 0,1% Vol. of Sample buffer. Ethidiumbromide intercalates into DNA, which makes it possible with UV Iluminator to visualize and fotograph stained DNA. Linear double-stranded DNA molecules are migrating through the gel according to their size. EcoRI and HindIII digested λ-DNA was used as a molecular weight standard.

Polymerase chain reaction (PCR)

Standard Polymerase chain reaction (Mullis et al., 1986) was performed in 0,5 l eppendorf containing 50 μl of total reaction mixture.

X μl DNA

5 μl 10x PCR-Buffer (with Mg^{2+})

2 μl dNTPs (each nucleotid 2 mM)

1,5 μl 5′-Primer (10 μM)

1,5 μl 3′-Primer (10 μM)

1 μl *PfuTurbo* DNA Polymerase (2,5 U/μl)

add to 50 μl H_2O

Standard amplification protocol (genomic DNA as a template)-35 cycles:

4 min → 94°C

30 sec → 94°C

30 sec → 60°C

4 min* → 72°C

6 min → 72°C

5 min → 4°C

* -Variable upon the length of the product

Standard amplification protocol for genotyping periostin-deficient mouse line-35 cycles:

3 min → 94°C

25 sec → 94°C

35 sec → 64°C

1 min → 72°C

6 min → 72°C

5 min → 4 °C

DNA sequencing

DNA sequencing was performed with „ABI-Prism-Dye-Cycle-Sequencing-Ready-Reaction Kit“ (Perkin Elmer) on ABI Prism 377 DNA-Sequencer (Perkin Elmer) at the sequencing facilities of Center for Molecular Neurobiology, Hamburg.

5.2.2 Cell Culture

Fibroblast cells

Primary embryonic fibroblasts cells (MEFs) were obtained from embryos that originate from crossings of homozygous, transgenic, neomycin-resistant mouse strain. These cells are known to support the growth of ES cells. Fibroblast cell were passaged several times and finally treated with Mitomycin C to arrest their growth. In 150 mm culture dish with 10 ml of culture media, 100 μl of Mitomycin C solution was added (1 mg/ml Mitomycin C in PBS, 5% DMSO, Sigma). After 2 h incubation at 37°C, cells were washed twice in PBS trypsinized and transferred to the new final cell culture dish. After allowing the neomycin resistant MEFs to attach these dishes, were then used to culture ES cells.

Embryonic stem cells

Frozen embryonic stem cells (ES) were thawed and co-cultured on mitotically inactivated mouse embryonic fibroblasts (feeder) (see above). They were closely monitored every day, subcultured and expanded until they reached optimal density. Approximately, $1x10^7$ ES cell have been mixed with 25-30 μg of linearized targeting vector and electroporated by applying 300V for 2msec (L. Fischer, Heidelberg) in an electroporation kuvette (Eurogentec, Belgium). Then, ES cells are resuspended and directly placed on 4 100mm feeder dishes. After allowing the electroporated cells to grow for 48 h in ES medium, the first (positive) selection with 400 μg/ml Geneticin (G418, Gibco) was started.

Two days later the second (negative) selection was started by addition of 2 μM Gancyclovir. Both drugs were present in the daily-renewed medium until they were isolated. Ideal colonies were isolated on the eighth day after electroporation with a micropipette in 15 μl PBS, dissociated in round-bottom 96-well plates with 30 μl trypsin (0,05% Trypsin/0,02% EDTA) and transferred onto previously prepared flat-bottom 96-well feeder plates. When the plates were circa 70% confluent, the culture was split. 25% of the cells were plated onto a new flat-bottom 96 well feeder plate and were after 1-2 days of growth cryopreserved in 10% DMSO; 10% FCS/ ES media. The remaining 75% were transferred onto a new flat-bottom 96-well plate that was previously coated with 0.5% gelatine/H_2O. After these clones were grown to confluency cells were lysed for DNA extraction and Southern analysis (see below).
After identification of correctly targeted ES cell clones, these colonies were thawed and placed onto 24-well dish for expansion. After another verification of the correct targeting event in theses cells by Southern Blot the cells were microinjected into C57/BL6 blastocysts.
Microinjection and implantation was done by the animal facility of the Center of Molecular Neurobiology.

96 well plate Screening procedure (Ramirez-Solis R., 1992) (Southern Blot)

The cells for DNA extraction were cultured until they reached confluence. Then they were lysed overnight at 55°C with 50 μl lysis buffer (10mM Tris-Hcl pH 7.5, 10 mM EDTA, 10 mM NaCl, 0.5% N-Lauroylsarcosin, 1 mg/ml ProteinaseK). Now the DNA was precipitated in 50 mM NaCl/ 96% EtOH, washed in 70%EtOH (3 times) and left to air dry for 10-20 minutes. In the mean time, a restriction digest mixture (1x restriction buffer, 5 μg/ml RNAse, 10-15 units of enzyme/sample, H_2O up to 35 μl) was prepared. DNA was digested overnight at 37°C. The next day, DNA was separated on 1% agarose gel and transferred by 20x SSC diffusion gradient to a

Nylonmenbrane (Hybond^{TM}-N+, Amersham) overnight. By UV-irradiation DNA was finally covalently linked to the membrane.

Radioactive DNA labelling and hybridization

The membrane with DNA was placed in prehybridization solution (6x SSC, 5x Denhardt's, 0.5% SDS, 100 μg/ml of denatured salmon sperm) for 30 min at 68°C in the water bath. For hybridization, the DNA probe was α-^{32}P-dCTP labelled (Feinberg et al., 1983) with "Prime-It Rmt Random Primer Labeling Kits" (Stratagene). The probe was purified on Sephadex G50-Microcolumn (Probe Quant G50, Amersham-Pharmacia) and denatured for 5 min at 95°C. Hybridization was carried out at 68°C overnight.

The next day, the membrane was washed (2x SSC, 0.5% SDS) twice for 30 min and finally exposed (Röntgenfilm, Kodak Biomax MR) at -80°C or developed overnight with PhosphoImagers (Fuji X-ray film, BAS 2000).

SDS-PAGE and Western Blot analysis

Protein concentration was determined by the Bradford protein assay and the same amounts were loaded on the polyacrylamide gel. Proteins were separated by the Laemmli method (Laemmli, 1970) and transferred from polyacrylamide gel onto a nitrocellulose membrane (Protran Nitrocellulose BA 85, 0,45 μm, Schleicher & Schüll) by the power supply set approximately 0.8 mA/cm2 of gel on the semy dry blotter (Bromma LKB, Sweden). The blotting sandwich was assembled as described in the manufactures protocol and the unstained marker (Bio-Rad) was used as a molecular weight marker. After protein transfer was completed, membranes were washed once in TBS and incubated in blocking buffer for 1 h at RT and the primary antibody (rabbit antiperiostin serum) was added in the 1:100 dillution overnight at 4°C. Aterwards, the membrane was washed 5x for 5 min in TBS and incubated with secondary antibody coupled with the horseradish peroxidase (HRP) (in 1:5000 dillution) for 1h at RT. Following the final washing in TBS, the immunoreactive bands were visualized using the enhanced chemiluminescence detection system (Pierce)

according to manufacturer instructions. The membrane was exposed to X-ray film (Biomax-MR, Kodak) for several time periods, starting with a 5 min exposure.

5.2.3 Isolation of genomic DNA from embryonic tissue and mouse tails for PCR reactions

Embryonic tissue and tails from adult mice were incubated in 150 µl of lysis buffer (10 mM Tris pH 8,5; 2,5 mM; 50 mM KCl; 0,45% Tween 20; 0,45% Igepal or Nonidet), constantly shaking at 55°C overnight. The next day, ProteinaseK was inactivated at 95°C for 10 min. 1 µl from this solution was used to set up the PCR reaction mixture for genotyping. The day of vaginal plug was taken as E0.

5.2.4 X-Gal staining

The whole embryos were fixed in 2% PFA for 2h at 4°C. After fixation and washing, embryos were incubated in detergent solution (0.1 M Phosphate buffer pH 7.3, 2 mM $MgCl_2$, 0.01% Natriumdesoxycholat, 0.02% Igepal or Nonidet P-40) for 10 min. Staining solution was prepared in detergent mixture (1 mg/ml X-Gal, 5 mM Potassiumferricyanid, 5 mM Potassiumferrocyanid) and staining was performed until the desired intensity of staining was achieved for a particular organ or tissue. Embryos were post-fixed in 4% PFA overnight and stored in 50% Glycerine/ PBS.

5.2.5 Tissue preparation for immunohistochemical analysis

For immunohistochemical analysis tissues were fixed in 2% PFA overnight at 4°C. The next day they were cryoprotected in 30% Sucrose for 24 h at 4°C and then

embedded with „Tissue Tec“ („OCT-Compound“; Nederland) in embedding boxes („Peel-Away“; Shandon, Frankfurt). This way prepared, tissue was stored at -80°C.

5.2.6 Immunostaining

Frozen tissue was cryosectioned (10 μm thickness). Sections were blocked with 0.1% PBT (Tween 20) containing 10% goat serum. Afterwards, they were incubated overnight with 1:700 rabbit anti-ß galactosidase (Abcam; Cambridge, UK) at 4°C.
After washing with PBT, sections were incubated with secondary antibodies conjugated to Alexa 466 or Cγ3 for 1h. Sections were carefully rinsed with PBS and nuclei were counterstained with 4′, 6′-diamidino-2-phenylindole (DAPI). Sections were then coated with mounting solution (Mowiol 4-88, Calbiochem) and analysed with Zeiss Axioplan microscope. Images were taken with the AxioCam digital camera (Zeiss).

5.2.7 Tissue preparation for histology analysis

The day of vaginal plug was defined as E0 and the day of birth defined as P0. Tissues were fixed overnight in 4% PFA and decalcified in 20% EDTA for 2 weeks. After dehydration in serial ethanol (30%, 50%, 70%, 80%, 96%, 2x 100%) they were incubated in a mixture of methylmetacrylate (Technovit 7100; Heraeus-Kulzer; Werheim) and 100% Ethanol (1:1) overnight. The next day tissue was infiltrated (100 ml Technovit 7100 with 1 g Hardner I) for 7 days. The tissue samples were finally embedded (Infiltration solution/Hardener II; 15:1) in a teflonform. After complete polymerization, the samples were glued with Technovit 3040 onto a carrier block and stored at room temperature.
Frontal and longitudinal 11 μm sections of mandibles were made on Microtome (Leica) and were placed on microscope slides (Roth). The haematoxylin/eosin

stained sections have been compared from apical to incisal direction with a light microscope (Zeiss).

5.2.8 Haematoxylin / Eosin staining

Tissue was stained with haematoxylin (Mayer's hemalaun) approximately 5 min and washed in tap water. Tissue was stained further with Eosin solution (0.4% Eosin Y/ H_2O) for circa 2 min and after washing in dH_2O it was allowed to dry at room temperature. Finally, tissue sections were covered with Eucitt (Kindler GmbH, Freiburg) and a coverslip.

5.2.9. Alizarin red staining

Skeletal preparations were made according to the alcian blue-alizarin red procedure, staining cartilage in blue and calcium–containing tissue in red. Newborn mice were eviscerated, fixed in 96% ethanol for four days, kept in acetone for three days and rinsed with water. For ten days, they were stained in staining solution containing 1 vol of 0,3% alcian blue (Sigma) in 70% ethanol, 1 vol of 0,1% alizarin red S (Sigma) in 95% ethanol, 1 vol of 100% acetic acid and 17 vol of ethanol. After rinsing, the specimens were kept in 20% glycerol-1% KOH at 37°C and then at room temperature until the tissue had completely cleared. Specimens were stored in 100% glycerol.

5.2.10 Scanning electron microscopy and Energy dispersive x-ray analysis (EDX)

Not decalcified postnatal mouse mandibular incisors were prepared as previously described for the histology analysis (see 5.2.7). Enamel rods have been made visible by acid etching (30 sec, 37 % phosphoric acid; Etching gel/ Ivoclar; Vivadent). All backscattered electron images were sampled from apical toward incisal zone from one of the mandibular incisors. Three pairs of homozygous and wild type mandibular incisors were compared. Scanning was performed by CamScan MaXim 2040S scanning microscope (Berlin, Germany).

To determine the content of Ca^{2+} and PO_4^{2-} ions in dental enamel and dentin, we used the same mandibular incisors and performed spectrophotometric analysis. Different regions of incisor surfaces from secretory, transition and maturation zones were measured. Measurements were performed for 100 sec on a defined surface of 80 μm-65 μm.

5.2.11 Eruption rate analysis

The mandibular incisors were marked with a trephine (Electronica, Imola, Italy) and photographed. The distance of the mark and a reference point, the gum margin, was determined. Due to the eruption process mark and reference point are separated with time. Measurements were performed each 5 days with 6 weeks old animals. To analyse the effect of different forms of nutrition on tooth eruption animals were fed powdered food (data not shown), soft pellet food, and hard pellet food. The same experiment was repeated with 16 months old animals that received hard and soft pellet food. Images were 1,6x magnified using a light microscope and examined by AxioCam Vision software. Mandibular incisors from 6 litters at P9 and P10 were examined to analyse the exact time of incisor penetration into the oral cavity.

5.2.12 Vickers hardness test

Mouse mandibular incisors were embedded in Technovit 7100. The surface of the blocks was ground with grinding SiC papers P-1200C and P4000C (Wirtz, Buehler, Düsseldorf). Final polishing was performed with a polish towel (VELTEX) and final polishing solution (0,1 um; pH 9,0). The Vickers hardness test method consists of indenting the material with a diamond indenter, in the form of a right pyramid with a square base and an angle of 136 degrees between opposite faces. The full load in

this study was applied for 20 sec. The two diagonals of the indentation left in the incisors surface after removal of the load, were measured using a microscope and their average values were calculated. The Vickers hardness test was performed on „Kleinlast härter prüfer“- miniload (Leica). Several measurements were performed on distinct, defined surfaces of the incisors. The load used, was 200p. The Vickers hardness was then calculated by dividing the load by the square area of indentation. Using specific tables the VH can be converted to kp/mm^2 values.

Abbreviations

μ	**Micro (10^{-6})**
°C	**Grad Celsius**
aa	**Amino acid**
ab	**Alveolar bone**
am	**Ameloblast**
AP	**Alkaline phosphatase**
d	**Dentin**
Da	**Dalton**
DL	**Dental folicle**
DMSO	**Dimethylsulfoxide**
DNA	**Deoxyribonucleic acid**
dNTP	**2'-desoxyribonucleotide-5'-triphosphate**
DRG	**Dorsal root ganglia**
e	**Enamel**
E. coli	**Escherichia coli**
EDTA	**Ethylendiamintetraacetic acid**
EMI	**Emi domain**
Fas	**Fasciclin domain**
FCS	**Fetal calf serum**
g	**Gram**
h	**Hour**
kb	**Kilo base pairs**
kDa	**Kilodalton**
LacZ	**ß-Galactosidase coding gene**
l	**Liter**
LB	**Luria Bertani**
M	**Molar**
m	**Mili**

MEM	**Minimal essential medium**
Min	**Minute**
mRNA	**Messenger ribonucleic acid**
Od	**Odontoblast**
P	**Pulp**
PAGE	**Polyacrylamide gel electrophoresis**
PDL	**Periodontal ligament**
PCR	**Polymerase chain reaction**
PFA	**Paraformaldehyde**
PBS	**Phosphat-buffered saline**
PNS	**Peripheral nervous system**
RNase	**Ribonuclease**
RT	**Room temperature**
SDS	**Sodium dodecyl sulfate**
Sr	**Stellate reticulum**
TK	**Thymidine kinase**
Tris	**Tris(-hydroxymethyl)-aminomethane**
v/v	**Volume per volume**
w/v	**Weight per volume**

References

Bae, J. S., Lee, S. H., Kim, J. E., Choi, J. Y., Park, R. W., Yong Park, J., Park, H. S., Sohn, Y. S., Lee, D. S., Bae Lee, E. et al. (2002). Betaig-h3 supports keratinocyte adhesion, migration, and proliferation through alpha3beta1 integrin. *Biochem Biophys Res Commun* 294, 940-8.

Bastiani, M. J., Harrelson, A. L., Snow, P. M. and Goodman, C. S. (1987). Expression of fasciclin I and II glycoproteins on subsets of axon pathways during neuronal development in the grasshopper. *Cell* 48, 745-55.

Beertsen, W. (1973). Tissue dynamics in the periodontal ligament of the mandibular incisor of the mouse: a preliminary report. *Arch Oral Biol* 18, 61-6.

Beertsen, W. (1975). Migration of fibroblasts in the periodontal ligament of the mouse incisor as revealed by autoradiography. *Arch Oral Biol* 20, 659-66.

Beertsen, W. and Everts, V. (1977). The site of remodeling of collagen in the periodontal ligament of the mouse incisor. *Anat Rec* 189, 479-97.

Beertsen, W., Everts, V. and van den Hooff, A. (1974). Fine structure of fibroblasts in the periodontal ligament of the rat incisor and their possible role in tooth eruption. *Arch Oral Biol* 19, 1087-98.

Beertsen, W., McCulloch, C. A. and Sodek, J. (1997). The periodontal ligament: a unique, multifunctional connective tissue. *Periodontol 2000* 13, 20-40.

Berkovitz, B. K. (1971). The effect of root transection and partial root resection on the unimpeded eruption rate of the rat incisor. *Arch Oral Biol* 16, 1033-43.

Berkovitz, B. K., Migdalski A., Solomon M. (1972). The effect of the lathyritic agent aminoacetonitrile on the unimpeded eruption rate in normal and root-resected rat lower incisors. *Archs oral Biol.* 17, 1755-1763.

Berkovitz, B. K. and Thomas, N. R. (1969). Unimpeded eruption in the root-resected lower incisor of the rat with a preliminary note on root transection. *Arch Oral Biol* 14, 771-80.

Billings, P. C., Herrick, D. J., Kucich, U., Engelsberg, B. N., Abrams, W. R., Macarak, E. J., Rosenbloom, J. and Howard, P. S. (2000). Extracellular matrix and nuclear localization of beta ig-h3 in human bladder smooth muscle and fibroblast cells. *J Cell Biochem* 79, 261-73.

Bosshardt, D. D. and Nanci, A. (1998). Immunolocalization of epithelial and mesenchymal matrix constituents in association with inner enamel epithelial cells. *J Histochem Cytochem* 46, 135-42.

Butler, P. M. (1995). Ontogenetic aspects of dental evolution. *Int J Dev Biol* 39, 25-34.

Cahill, D. R. and Marks, S. C., Jr. (1980). Tooth eruption: evidence for the central role of the dental follicle. *J Oral Pathol* 9, 189-200.

Cotton, W. R. a. G., J.F. (1974). Unerupted dentition secondary to congenital osteopetrosis in the Osborne-Mendel rat. *Proc Soc Exp Biol Med* 146, 554-561.

Doliana, R., Bot, S., Bonaldo, P. and Colombatti, A. (2000). EMI, a novel cysteine-rich domain of EMILINs and other extracellular proteins, interacts with the gC1q domains and participates in multimerization. *FEBS Lett* 484, 164-8.

Eccles, J. D. (1965). The effects of reducing function and stopping eruption on the periodontium of the rat incisor. *J Dent Res* 44, 860-8.

Elkins, T., Hortsch, M., Bieber, A. J., Snow, P. M. and Goodman, C. S. (1990). Drosophila fasciclin I is a novel homophilic adhesion molecule that along with fasciclin III can mediate cell sorting. *J Cell Biol* 110, 1825-32.

Everts, V. a. B. W. (1988). The cellular basis of tooth eruption. *The Biological Mechanisms of Tooth Eruption and Root Resorption*, 237-242.

Ferguson, J. W., Thoma, B. S., Mikesh, M. F., Kramer, R. H., Bennett, K. L., Purchio, A., Bellard, B. J. and LeBaron, R. G. (2003). The extracellular matrix protein betaIG-H3 is expressed at myotendinous junctions and supports muscle cell adhesion. *Cell Tissue Res* 313, 93-105.

Fujita, T., Shiba, H., Sakata, M., Uchida, Y., Nakamura, S. and Kurihara, H.(2002).SPARC stimulates the synthesis of OPG/OCIF, MMP-2 and DNA inhuman periodontal ligament cells. *J Oral Pathol Med* 31, 345-52.

Gillan, L., Matei, D., Fishman, D. A., Gerbin, C. S., Karlan, B. Y. and Chang, D. D. (2002). Periostin secreted by epithelial ovarian carcinoma is a ligand for alpha(V)beta(3) and alpha(V)beta(5) integrins and promotes cell motility. *Cancer Res* 62, 5358-64.

Halse, A. (1973). Effect of dietary iron deficiency on the pigmentation and iron content of rat incisor enamel. *Scand J Dent Res* 81, 319-34.

Halse, A. (1974). The mineral phase of rodent incisor enamel with special reference to the iron-containing layer. *Nor Tannlaegeforen Tid* 84, 138-43.

Halse, A. and Selvig, K. A. (1974). Incorporation of iron in rat incisor enamel. *Scand J Dent Res* 82, 47-56.

Harada, H., Kettunen, P., Jung, H. S., Mustonen, T., Wang, Y. A. and Thesleff, I. (1999). Localization of putative stem cells in dental epithelium and their association with Notch and FGF signaling. *J Cell Biol* 147, 105-20.

Harada, H., Mitsuyasu, T., Toyono, T. and Toyoshima, K. (2002). Epithelial stem cells in teeth. *Odontology* 90, 1-6.

Herzberg, F., and I. Schour. (1941). Effects of the removal of pulps and Hertwig's sheat on the eruption of incisors in the albino rat. *J.Dent.Res.* 20, 264.

Horiuchi, K., Amizuka, N., Takeshita, S., Takamatsu, H., Katsuura, M., Ozawa, H., Toyama, Y., Bonewald, L. F. and Kudo, A. (1999). Identification and characterization of a novel protein, periostin, with restricted expression to periosteum and periodontal ligament and increased expression by transforming growth factor beta. *J Bone Miner Res* 14, 1239-49.

Howard, P. S., Kucich, U., Taliwal, R. and Korostoff, J. M. (1998). Mechanical forces alter extracellular matrix synthesis by human periodontal ligament fibroblasts. *J Periodontal Res* 33, 500-8.

Hu, S., Sonnenfeld, M., Stahl, S. and Crews, S. T. (1998). Midline Fasciclin: a Drosophila Fasciclin-I-related membrane protein localized to the CNS midline cells and trachea. *J Neurobiol* 35, 77-93.

Huber, O. and Sumper, M. (1994). Algal-CAMs: isoforms of a cell adhesion molecule in embryos of the alga Volvox with homology to Drosophila fasciclin I. *Embo J* 13, 4212-22.

Jeong, H. W. and Kim, I. S. (2004). TGF-beta1 enhances betaig-h3-mediated keratinocyte cell migration through the alpha3beta1 integrin and PI3K. *J Cell Biochem* 92, 770-80.

Jernvall, J. and Thesleff, I. (2000). Reiterative signaling and patterning during mammalian tooth morphogenesis. *Mech Dev* 92, 19-29.

Kallenbach, E. (1970). Fine structure of rat incisor enamel organ during late pigmentation and regression stages. *J Ultrastruct Res* 30, 38-63.

Kapila, Y. L., Lancero, H. and Johnson, P. W. (1998). The response of periodontal ligament cells to fibronectin. *J Periodontol* 69, 1008-19.

Kawamoto, T., Noshiro, M., Shen, M., Nakamasu, K., Hashimoto, K., Kawashima-Ohya, Y., Gotoh, O. and Kato, Y. (1998). Structural and phylogenetic analyses of RGD-CAP/beta ig-h3, a fasciclin-like adhesion protein expressed in chick chondrocytes. *Biochim Biophys Acta* 1395, 288-92.

Keranen, S. V., Kettunen, P., Aberg, T., Thesleff, I. and Jernvall, J. (1999). Gene expression patterns associated with suppression of odontogenesis in mouse and vole diastema regions. *Dev Genes Evol* 209, 495-506.

Kern, C. B., Hoffman, S., Moreno, R., Damon, B. J., Norris, R. A., Krug, E. L., Markwald, R. R. and Mjaatvedt, C. H. (2005). Immunolocalization of chick periostin protein in the developing heart. *Anat Rec A Discov Mol Cell Evol Biol* 284, 415-23.

Kii, I., Amizuka, N., Minqi, L., Kitajima, S., Saga, Y. and Kudo, A. (2006). Periostin is an extracellular matrix protein required for eruption of incisors in mice. *Biochem Biophys Res Commun* 342, 766-72.

Kim, J. E., Kim, S. J., Jeong, H. W., Lee, B. H., Choi, J. Y., Park, R. W., Park, J. Y. and Kim, I. S. (2003). RGD peptides released from beta ig-h3, a TGF-beta-induced cell-adhesive molecule, mediate apoptosis. *Oncogene* 22, 2045-53.

Kim, J. E., Kim, S. J., Lee, B. H., Park, R. W., Kim, K. S. and Kim, I. S. (2000). Identification of motifs for cell adhesion within the repeated domains of transforming growth factor-beta-induced gene, betaig-h3. *J Biol Chem* 275, 30907-15.

Kollar, E. J. and Lumsden, A. G. (1979). Tooth morphogenesis: the role of the innervation during induction and pattern formation. *J Biol Buccale* 7, 49-60.

Kruzynska-Frejtag, A., Machnicki, M., Rogers, R., Markwald, R. R. and Conway, S. J. (2001). Periostin (an osteoblast-specific factor) is expressed within the embryonic mouse heart during valve formation. *Mech Dev* 103, 183-8.

Kruzynska-Frejtag, A., Wang, J., Maeda, M., Rogers, R., Krug, E., Hoffman, S., Markwald, R. R. and Conway, S. J. (2004). Periostin is expressed within the developing teeth at the sites of epithelial-mesenchymal interaction. *Dev Dyn* 229, 857-68.

Kudo, H., Amizuka, N., Araki, K., Inohaya, K. and Kudo, A. (2004). Zebrafish periostin is required for the adhesion of muscle fiber bundles to the myoseptum and for the differentiation of muscle fibers. *Dev Biol* 267, 473-87.

Kuhn R., R. K., Muller W. (1991). Generation and analysis of interleukin-4 deficient mice. *Science* 254, 707-710.

Lavelle, C. L. (1969). The effect of age on the eruption rate of the incisor teeth of the rat (Rattus norvegicus). *J Anat* 104, 109-16.

LeBaron, R. G., Bezverkov, K. I., Zimber, M. P., Pavelec, R., Skonier, J. and Purchio, A. F. (1995). Beta IG-H3, a novel secretory protein inducible by transforming growth factor-beta, is present in normal skin and promotes the adhesion and spreading of dermal fibroblasts in vitro. *J Invest Dermatol* 104, 844-9.

Li, G., Oparil, S., Sanders, J. M., Zhang, L., Dai, M., Chen, L. B., Conway, S. J.,McNamara, C. A. and Sarembock, I. J. (2005). Phosphatidylinositol-3-kinase signaling mediates vascular smooth muscle cell expression of periostin in vivo and in vitro. ***Atherosclerosis*****.**

Lindner, V., Wang, Q., Conley, B. A., Friesel, R. E. and Vary, C. P. (2005).Vascular injury induces expression of periostin: implications for vascular cell differentiation and migration. ***Arterioscler Thromb Vasc Biol*** **25, 77-83.**

Litvin, J., Blagg, A., Mu, A., Matiwala, S., Montgomery, M., Berretta, R., Houser, S. and Margulies, K. (2006). Periostin and periostin-like factor in the human heart: possible therapeutic targets. ***Cardiovasc Pathol*** **15, 24-32.**

Litvin, J., Selim, A. H., Montgomery, M. O., Lehmann, K., Rico, M. C., Devlin, H., Bednarik, D. P. and Safadi, F. F. (2004). Expression and function of periostin-isoforms in bone. ***J Cell Biochem*** **92, 1044-61.**

Litvin, J., Zhu, S., Norris, R. and Markwald, R. (2005). Periostin family of proteins: Therapeutic targets for heart disease. ***Anat Rec A Discov Mol Cell Evol Biol*** **287A, 1205-1212.**

Luckett, W. P. and Maier, W. (1982). Development of deciduous and permanent dentition in Tarsius and its phylogenetic significance. ***Folia Primatol (Basel)*** **37, 1-36.**

MacDougall, M., Gu, T. T., Luan, X., Simmons, D. and Chen, J. (1998). Identification of a novel isoform of mouse dentin matrix protein 1: spatial expression in mineralized tissues. ***J Bone Miner Res*** **13, 422-31.**

Main. (1966). Experiments on the rat incisor into the cellular proliferation and blood-pressure theories of tooth eruption. ***Arch Oral Biol*** **2, 163-178.**

Marks, S. C., Jr. (1973). Pathogenesis of osteopetrosis in the ia rat: reduced bone resorption due to reduced osteoclast function. ***Am J Anat*** **138, 165-89.**

Marks, S. C., Jr. (1977). Osteopetrosis in the toothless (t1) rat: presence of osteoclasts but failure to respond to parathyroid extract or to be cured by infusion of spleen or bone marrow cells from normal littermates. ***Am J Anat*** **149, 289-97.**

Marks, S. C., Jr. and Cahill, D. R. (1987). Regional control by the dental follicle of alterations in alveolar bone metabolism during tooth eruption. *J Oral Pathol* 16, 164-9.

Marks, S. C., Jr., Cahill, D. R. and Wise, G. E. (1983). The cytology of the dental follicle and adjacent alveolar bone during tooth eruption in the dog. *Am J Anat* 168, 277-89.

Marks, S. C., Jr. and Schroeder, H. E. (1996). Tooth eruption: theories and facts. *Anat Rec* 245, 374-93.

Massler, M., and I. Schour. (1941). Studies in tooth development: Teories of eruption. *Am.J.Orthodont.Oral Surg.* 27, 552-576.

Melcher, A. H. (1967). Remodelling of the periodontal ligament during eruption of the rat incisor. *Arch Oral Biol* 12, 1649-51.

Nam, J. O., Kim, J. E., Jeong, H. W., Lee, S. J., Lee, B. H., Choi, J. Y., Park, R. W., Park, J. Y. and Kim, I. S. (2003). Identification of the alphavbeta3 integrin-interacting motif of betaig-h3 and its anti-angiogenic effect. *J Biol Chem* 278, 25902-9.

Narayanan AS., H. T. (1985). Characterization of collagens in phenytoin-enlarged human gingiva. *Coll Relat Res* 5, 513-518.

Ness, A. R. (1965). Eruption rates of impeded and unimpeded mandibular incisors of the adult laboratory mouse. *Arch Oral Biol* 10, 439-51.

Norris, R. A., Kern, C. B., Wessels, A., Moralez, E. I., Markwald, R. R. and Mjaatvedt, C. H. (2004). Identification and detection of the periostin gene in cardiac development. *Anat Rec A Discov Mol Cell Evol Biol* 281, 1227-33.

Ohno, S., Doi, T., Tsutsumi, S., Okada, Y., Yoneno, K., Kato, Y. and Tanne, K.(2002). RGD-CAP ((beta)ig-h3) is expressed in precartilage condensation and in prehypertrophic chondrocytes during cartilage development. *Biochim Biophys Acta* 1572, 114-22.

Park, S. W., Bae, J. S., Kim, K. S., Park, S. H., Lee, B. H., Choi, J. Y., Park, J. Y., Ha, S. W., Kim, Y. L., Kwon, T. H. et al. (2004). Beta ig-h3 promotes renal proximal tubular epithelial cell adhesion, migration and proliferation through the interaction with alpha3beta1 integrin. *Exp Mol Med* 36, 211-9.

Perl, T. and Farman, A. G. (1977). Radicular (type 1) dentin dysplasia. *Oral Surg Oral Med Oral Pathol* 43, 746-53.

Peterkova, R. (1985). The common developmental origin and phylogenetic aspects of teeth, rugae palatinae, and fornix vestibuli oris in the mouse. *J Craniofac Genet Dev Biol* 5, 89-104.

Pitaru, S., Aubin, J. E., Bhargava, U. and Melcher, A. H. (1987). Immunoelectron microscopic studies on the distributions of fibronectin and actin in a cellular dense connective tissue: the periodontal ligament of the rat. *J Periodontal Res* 22, 64-74.

Ramirez-Solis R., R.-P. J., Wallace JD., Wims M., Zheng H., Bradley A. (1992). Genomic DNA microextraction: a method to screen numerous samples. *Anal Biochem.* 201, 331-335.

Rios, H., Koushik, S. V., Wang, H., Wang, J., Zhou, H. M., Lindsley, A., Rogers, R., Chen, Z., Maeda, M., Kruzynska-Frejtag, A. et al. (2005). periostin null mice exhibit dwarfism, incisor enamel defects, and an early-onset periodontal disease-like phenotype. *Mol Cell Biol* 25, 11131-44.

Robinson, C., Brookes, S. J., Shore, R. C. and Kirkham, J. (1998). The developing enamel matrix: nature and function. *Eur J Oral Sci* 106 Suppl 1, 282-91.

Robinson, C., Kirkham, J., Brookes, S. J., Bonass, W. A. and Shore, R. C. (1995). The chemistry of enamel development. *Int J Dev Biol* 39, 145-52.

Ruch, J. V. (1987). Determinisms of odontogenesis. *Revis Biol Celular* 14, 1-99.

Ruch, J. V., Karcher-Djuricic, V. and Gerber, R. (1972). [Several aspects of the predentin role in the differentiation of ameloblasts]. *Arch Anat Microsc Morphol Exp* 61, 127-38.

Sakakura, Y., Fujiwara, N. and Nawa, T. (1989). Epithelial cytodifferentiation and extracellular matrix formation in enamel-free areas of the occlusal cusp during development of mouse molars: light and electron microscopic studies. *Am J Anat* 184, 287-97.

Schour. (1934). The Hypophysis and the Teeth. *The Angle Orthodontist* IV, 3-21.

Schroeder, H. E., Luder, H. U. and Bosshardt, D. D. (1992). Morphological and labeling evidence supporting and extending a modern theory of tooth eruption. *Schweiz Monatsschr Zahnmed* 102, 20-31.

Seifert, M. F., Popoff, S. N. and Marks, S. C., Jr. (1988). Skeletal biology in the toothless (osteopetrotic) rat. *Am J Anat* 183, 158-65.

Shields, E. D., Bixler, D. and el-Kafrawy, A. M. (1973). A proposed classification for heritable human dentine defects with a description of a new entity. *Arch Oral Biol* 18, 543-53.

Sicher, H. (1942). Tooth eruption. *J.Dent.Res.* 21, 201-210.

Skonier, J., Neubauer, M., Madisen, L., Bennett, K., Plowman, G. D. and Purchio, A. F. (1992). cDNA cloning and sequence analysis of beta ig-h3, a novel gene induced in a human adenocarcinoma cell line after treatment with transforming growth factor-beta. *DNA Cell Biol* 11, 511-22.

Smith, C. E. (1998). Cellular and chemical events during enamel maturation. *Crit Rev Oral Biol Med* 9, 128-61.

Smith, C. E. and Warshawsky, H. (1975). Histological and three dimensional

organization of the odontogenic organ in the lower incisor of 100 gram rats. *Am J Anat* 142, 403-29.

Smith, J. C., Symes, K., Hynes, R. O. and DeSimone, D. (1990). Mesoderm induction and the control of gastrulation in Xenopus laevis: the roles of fibronectin and integrins. *Development* 108, 229-38.

Sodek, J. and Ferrier, J. M. (1988). Collagen remodelling in rat periodontal tissues: compensation for precursor reutilization confirms rapid turnover of collagen. *Coll Relat Res* 8, 11-21.

Stock, D. W., Weiss, K. M. and Zhao, Z. (1997). Patterning of the mammalian dentition in development and evolution. *Bioessays* 19, 481-90.

Sutton, P. R. and Graze, H. R. (1985). The blood-vessel thrust theory of tooth eruption and migration. *Med Hypotheses* 18, 289-95.

Takeshita, S. (1993). Osteoblast-specific factor 2: cloning of a putative bone adhesion protein with homology with the insect protein fasciclin I. *Biochem J* 294, 271-278.

Ten Cate, A. R., Deporter, D. A. and Freeman, E. (1976). The role of fibroblasts in the remodeling of periodontal ligament during physiologic tooth movement. *Am J Orthod* 69, 155-68.

Thesleff, I. (2000). Genetic basis of tooth development and dental defects. *Acta Odontol Scand* 58, 191-4.

Thesleff, I. and Aberg, T. (1997). Tooth morphogenesis and the differentiation of ameloblasts. *Ciba Found Symp* 205, 3-12; discussion 12-7.

Thesleff, I. and Hurmerinta, K. (1981). Tissue interactions in tooth development. *Differentiation* 18, 75-88.

Tomakidi, P., Fusenig, N. E., Kohl, A. and Komposch, G. (1997). Histomorphological and biochemical differentiation capacity in organotypic co-cultures of primary gingival cells. *J Periodontal Res* 32, 388-400.

Tucker, A. and Sharpe, P. (2004). The cutting-edge of mammalian development; how the embryo makes teeth. *Nat Rev Genet* 5, 499-508.

Uitto, V. J. and Larjava, H. (1991). Extracellular matrix molecules and their receptors: an overview with special emphasis on periodontal tissues. *Crit Rev Oral Biol Med* 2, 323-54.

Ulstrup, J. C., Jeansson, S., Wiker, H. G. and Harboe, M. (1995). Relationship of secretion pattern and MPB70 homology with osteoblast-specific factor 2 to osteitis following Mycobacterium bovis BCG vaccination. *Infect Immun* 63, 672-5.

Wessels, A. and Sedmera, D. (2003). Developmental anatomy of the heart: a tale of mice and man. *Physiol Genomics* 15, 165-76.

Wilde, J., Yokozeki, M., Terai, K., Kudo, A. and Moriyama, K. (2003). The divergent expression of periostin mRNA in the periodontal ligament during experimental tooth movement. *Cell Tissue Res* 312, 345-51.

Wise, G. E., Frazier-Bowers, S. and D'Souza, R. N. (2002). Cellular, molecular, and genetic determinants of tooth eruption. *Crit Rev Oral Biol Med* 13, 323-34.

Yoshioka, N., Fuji, S., Shimakage, M., Kodama, K., Hakura, A., Yutsudo, M., Inoue, H. and Nojima, H. (2002). Suppression of anchorage-independent growth of human cancer cell lines by the TRIF52/periostin/OSF-2 gene. *Exp Cell Res* 279, 91-9.

Zinn, K., McAllister, L. and Goodman, C. S. (1988). Sequence analysis and neuronal expression of fasciclin I in grasshopper and Drosophila. *Cell* 53, 577-87.

Acknowledgements

This study has been performed in the Center for Molecular Neurobiology Hamburg (ZMNH) at the University of Hamburg. I would like to thank Dr. Dieter Riethmacher for giving me the opportunity to perform my Ph.D. research in his laboratory.

Also, I would like to thank Prof. Thomas Jentsch (ZMNH, University of Hamburg) and Prof. Ulrich Hahn (Department of Chemistry, University of Hamburg) for the supervision of my Ph.D. thesis.

I also wish to thank the present and former colleagues in the lab and the members of the other research groups at the ZMNH for their help during this work.

I am especially grateful to Prof. Colin Robinson (Leeds Dental Institute, Division of Oral Biology, Leeds, UK) for his suggestions regarding the analysis of the tooth phenotype. I also thank our collaborator Prof. Ralf Radlanski (Department of Oral Structural Biology, University of Berlin) who made it possible to perform the SEM, and EDX analysis in his laboratory, as well as the Vickers Hardness test.

Last but not least, I would like to thank all my friends for their friendship and understanding and my family in Croatia for their support and love.

Eidesstattliche Versicherung

Hiermit erkläre ich, Frau Andreja Brodarac, in Kenntnis der Strafbarkeit einer falschen Eidesstattlichen Versicherung, folgendes an Eides Statt:

Meine vorliegende Dissertationsschrift wurde von mir selbständig und ohne fremde Hilfe angefertigt.

Hamburg, den 22.05.06